Supporting Information

SI1. Synthetic protocols

SI2. Key parameters concerning the TT derivatives estimated by DFT computations

SI3. Supplementary Absorption/Emission/Lifetime spectra

SI4. Supplementary Electrochemical/Spectroelectrochemical data

SI1.1. *Synthesis of 3-(thiophen-2-yl)triimidazo[1,2-a:1',2'-c:1'',2''-e][1,3,5]triazine* **(2-Th)TT**

(2-Th)TT was prepared by Stille coupling between **BrTT** and 2-(tributylstannyl)thiophene (see **Scheme S1.1**).

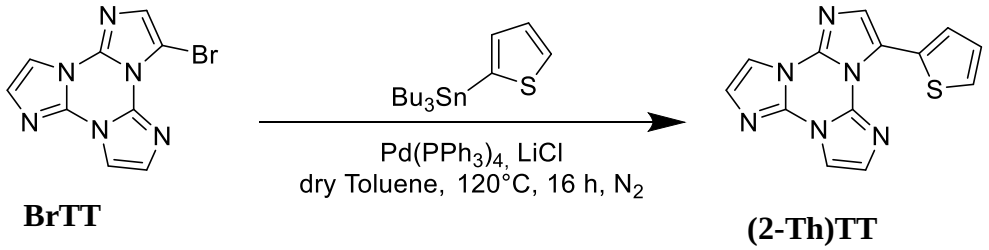

BrTT **(2-Th)TT**

Scheme SI1.1. Synthetic path for the preparation of **(2-Th)TT**

In a typical reaction, **BrTT** (0.250 g; 0.902 mmol), 2-(tributylstannyl)thiophene (0.315 mL, 0.992 mmol), LiCl (0.382 g, 9.202 mmol), $Pd(PPh_3)_4$ (0.104 g, 0.091 mmol) and dry toluene (15 mL) were transferred inside a dried 100 mL Schlenk flask equipped with a magnetic stirrer and three freeze-pump-thaw cycles were performed. The system was heated under static nitrogen atmosphere at 120 °C for 16 h. The reaction was then cooled to room temperature, diluted with CH_2Cl_2 (50 mL) and filtered on a Büchner with filter paper. The crude reaction mixture was evaporated to dryness and further purified by flash chromatography on SiO_2 with CH_2Cl_2/MeCN as eluents to give **(2-Th)TT** as a white solid (0.170 g, 67% Yield, R_f = 0.3 in CH_2Cl_2/MeCN = 8/2). Before performing the spectroscopic and electrochemical characterization, the product was further purified by crystallization from DCM/MeOH.

NMR data (9.4 T, DMSO-d_6, 298 K, δ, ppm): ^{1}H NMR 7.98 (d, J = 1.7 Hz, 1H), 7.97 (d, J = 1.7 Hz, 1H), 7.76 (dd, J = 3.6, 1.1 Hz, 1H), 7.67 (dd, J = 5.1, 1.0 Hz, 1H), 7.40 (s, 1H), 7.29 (d, J = 1.7 Hz, 1H), 7.25 (d, J = 1.7 Hz, 1H), 7.23 – 7.16 (dd, J = 3.6, 5.1 Hz, 1H). **^{13}C NMR** 137.06 (C), 136.25 (C), 136.02 (C), 130.22 (CH), 128.98 (CH), 128.81 (C), 128.39 (CH), 127.86 (CH), 127.70 (CH), 121.77 (C), 112.19 (CH), 111.82 (CH) (Figures S1-S2).

MS (ESI-positive ion mode): *m/z*: 280.95 $[M+H]^+$ (Figure S3).

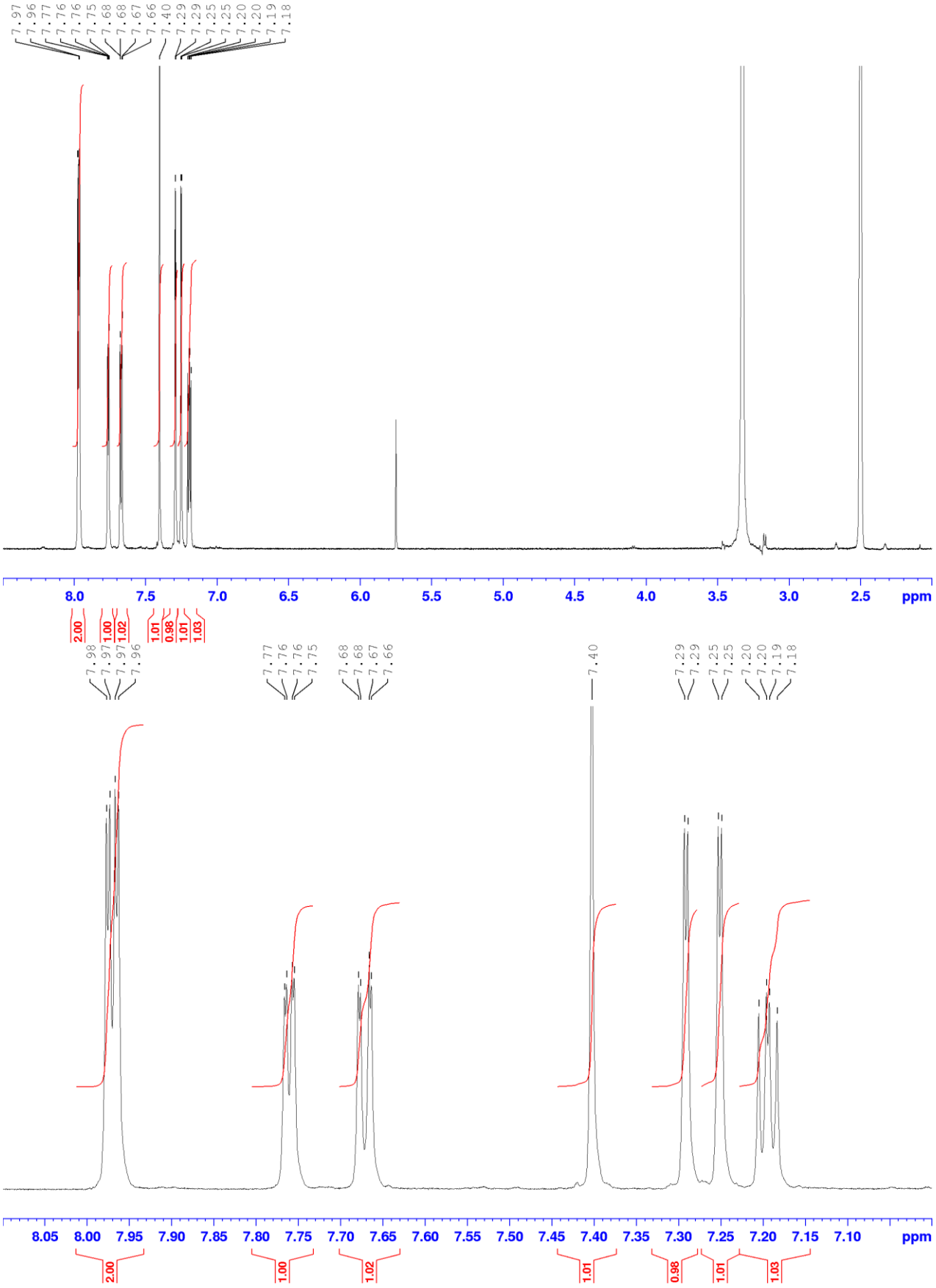

Figure S1. ^{1}H NMR spectrum of **(2-Th)TT** (400 MHz, DMSO-d_6, top) with expansion of aromatic region (bottom).

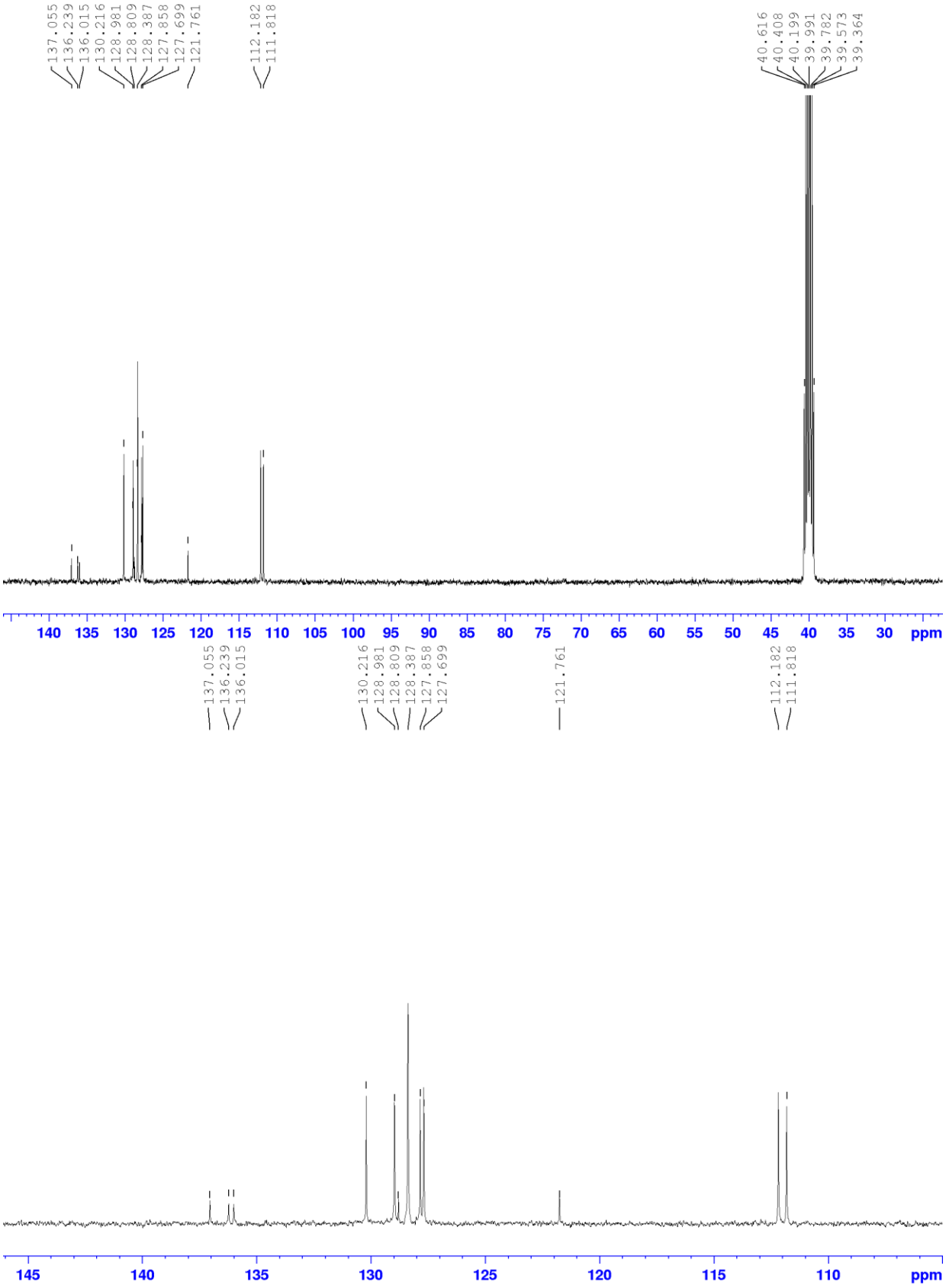

Figure S2. ^{13}C NMR spectrum of **(2-Th)TT** (100 MHz, DMSO-d_6, top) with expansion of aromatic region (bottom).

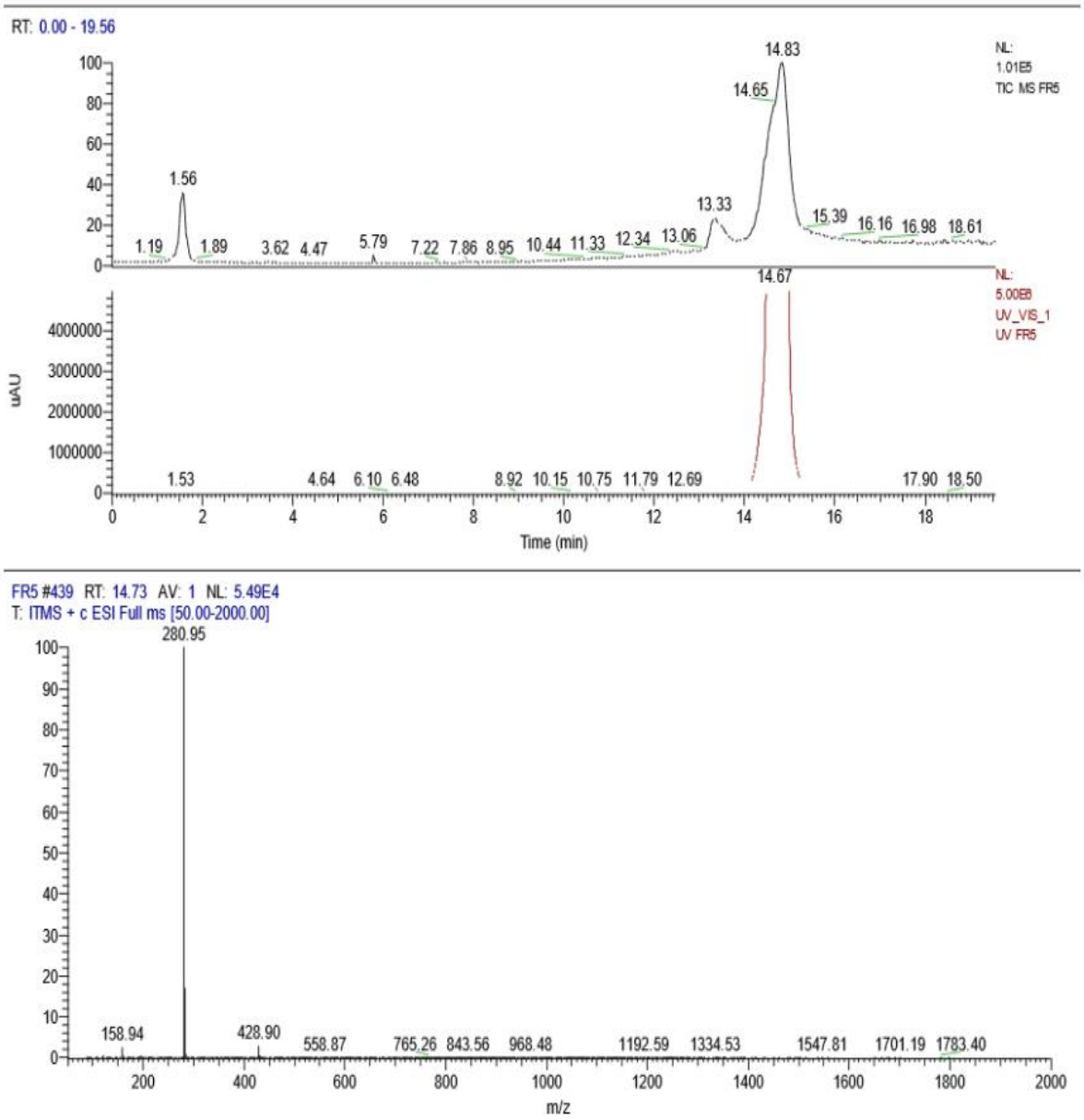

Figure S3: LC-MS profile of **(2-Th)TT**.

SI1.2 *Synthesis of 3,7-di(thiophen-2-yl)triimidazo[1,2-a:1',2'-c:1'',2''-e][1,3,5]triazine* **(2-Th)$_2$TT**

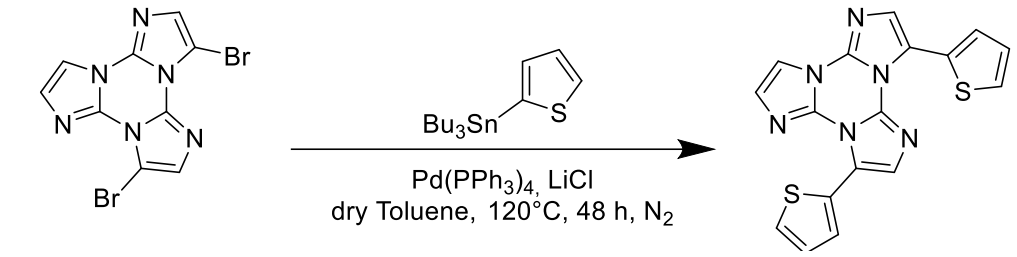

Br$_2$TT **(2-Th)$_2$TT**

Scheme SI1.2 Synthetic path for the preparation of **(2-Th)$_2$TT**

(2-Th)$_2$TT was prepared by Stille coupling between **Br$_2$TT** and 2-(tributylstannyl)thiophene (see Scheme SI1.2). In a typical reaction, **Br$_2$TT** (0.300 g; 0.843 mmol), 2-(tributylstannyl)thiophene (1.00 mL, 3.371 mmol), CuO (0.302 mg, 3.793 mmol), $Pd(PPh_3)_2Cl_2$ (0.059 g, 0.084 mmol) and dry toluene (10 mL) were transferred inside a dried 100 mL Schlenk flask equipped with a magnetic stirrer and three freeze-pump-thaw cycles were performed. The system was heated under static nitrogen atmosphere at 120 °C for 48 h. The reaction was then cooled to room temperature, diluted with 50 mL of CH_2Cl_2 and filtered on Celite. The organic phase was evaporated in vacuum and the solid crude reaction mixture was further purified by automated flash chromatography on SiO_2 with Hexane/AcOEt as eluents to give the **(2-Th)$_2$TT** product as a white solid (0.543 g, 63% Yield, R_f = 0.65 in Hexane/AcOEt = 7/3).

NMR data (9.4 T, CD_2Cl_2, 298 K, δ, ppm): ^{1}H NMR 7.82 (d, J = 1.6 Hz, 1H), 7.65 (m, 2H), 7.50 (m, 2H), 7.29 (s, 1H), 7.24 – 7.15 (m, 5H). **^{13}C NMR** 136.56 (C), 136.38 (C), 135.79 (C), 130.97 (CH), 130.88 (CH), 129.67 (CH), 129.25 (CH), 129.12 (CH), 128.61 (C), 128.48 (C), 127.73 (CH), 127.69 (CH), 122.46 (C), 121.92 (C), 111.61 (CH) (Figures S4-S5).
MS (ESI-positive ion mode): *m/z*: 363.20 $[M+H]^+$ (Figure S6).

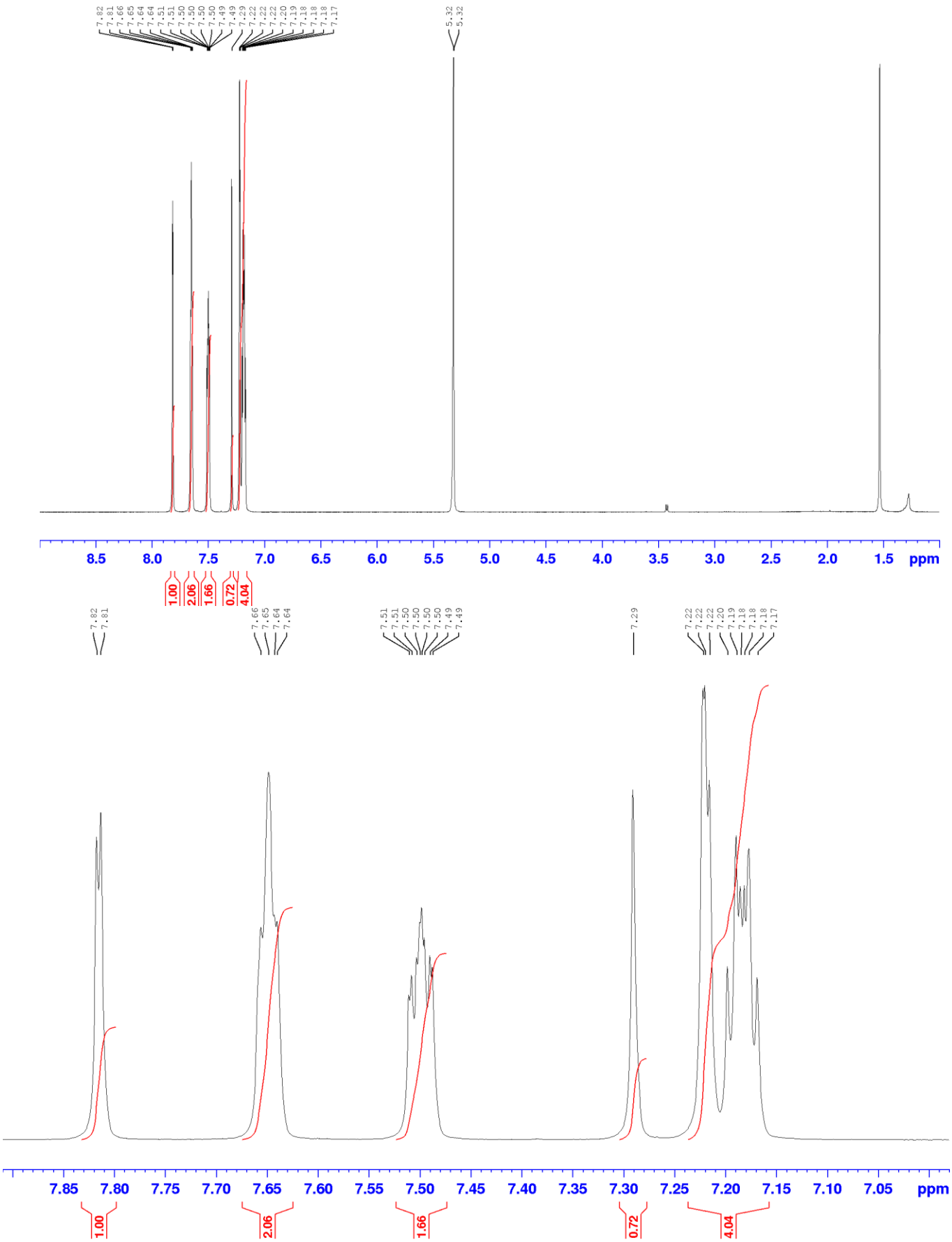

Figure S4. ^{1}H NMR spectrum of **(2-Th)$_2$TT** (400 MHz, CD_2Cl_2, top) with expansion of aromatic region (bottom).

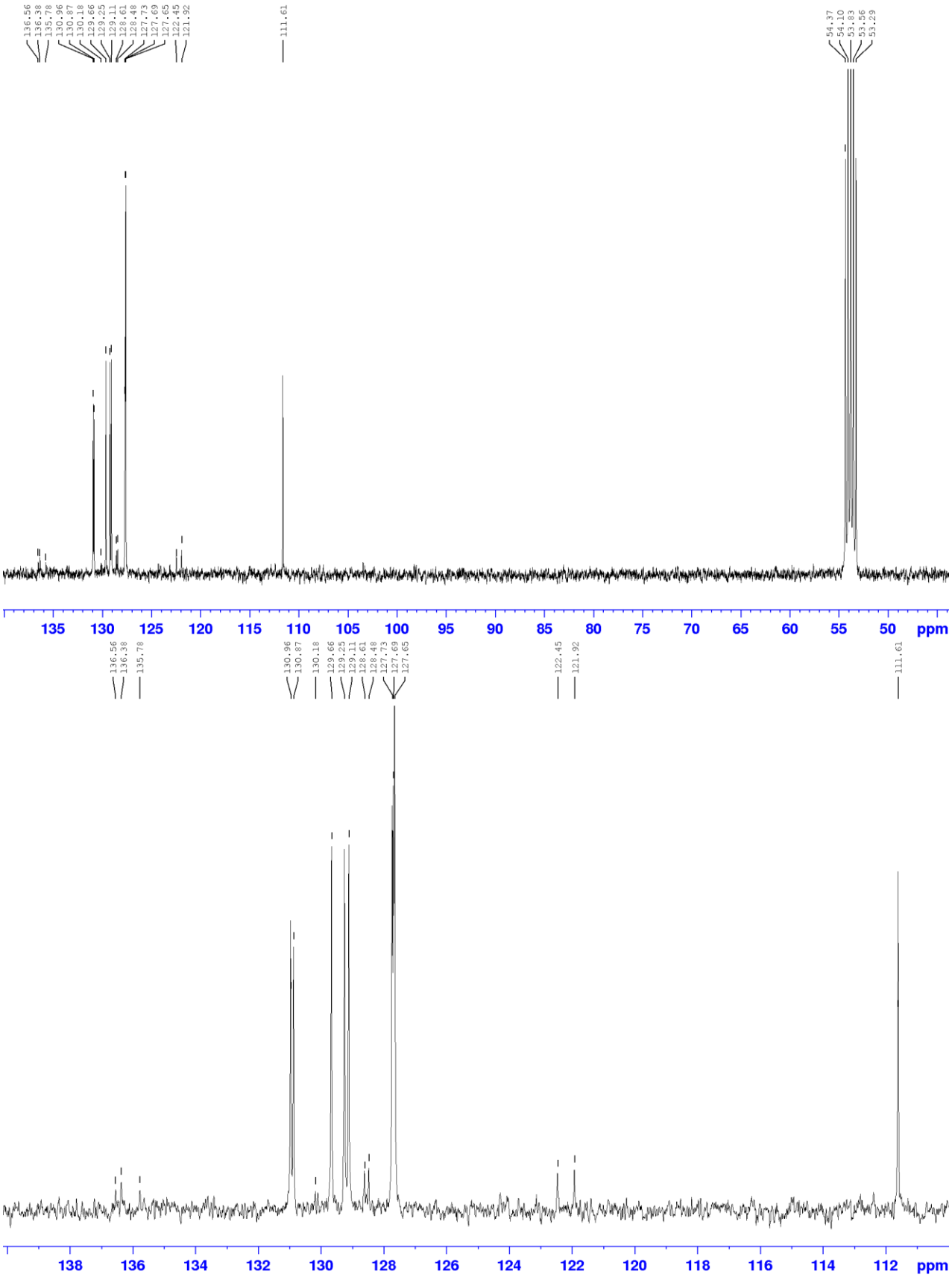

Figure S5. ^{13}C NMR spectrum of **(2-Th)$_2$TT** (100 MHz, CD_2Cl_2, top) with expansion of aromatic region (bottom).

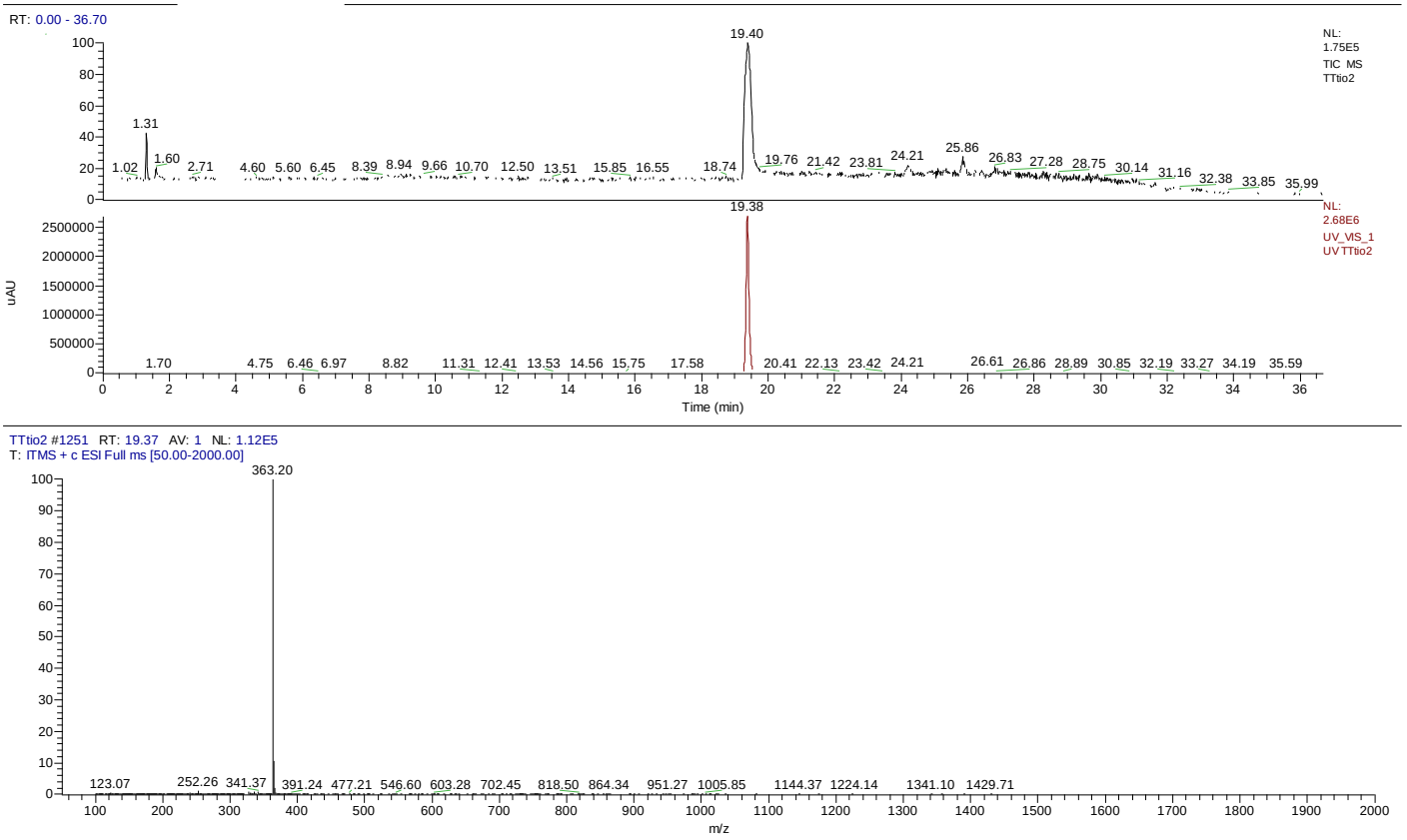

Figure S6: LC-MS profile of **(2-Th)$_2$TT**.

SI1.3 *Synthesis of 3,7,11-tri(thiophen-2-yl)triimidazo[1,2-a:1',2'-c:1",2"-e][1,3,5]triazine* **(2-Th)$_3$TT**

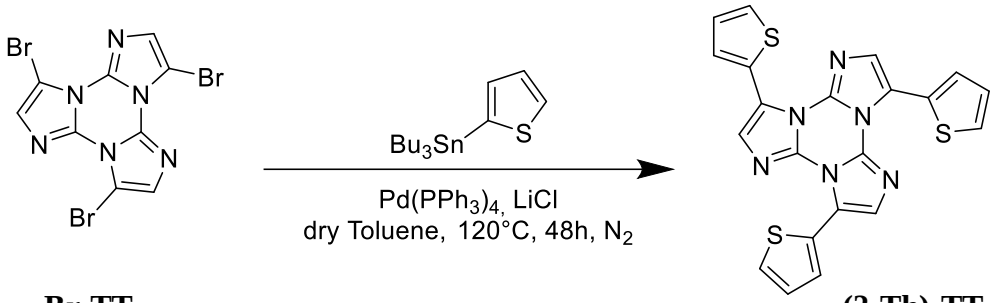

Br$_3$TT **(2-Th)$_3$TT**

Scheme SI1.3. Synthetic path for the preparation of **(2-Th)$_3$TT**

(2-Th)$_3$TT was prepared by Stille coupling between **Br$_3$TT** and 2-(tributylstannyl)thiophene. In a typical reaction, **Br$_3$TT** (0.200 g; 0.460 mmol), 2-(tributylstannyl)thiophene (0.730 mL, 2.29 mmol), LiCl (0.636 mg, 4.60 mmol), $Pd(PPh_3)_2Cl_2$ (0.0323 g, 0.046 mmol) and dry toluene (10 mL) were transferred inside a dried 100 mL Schlenk flask equipped with a magnetic stirrer and three freeze-pump-thaw cycles were performed. The system was heated under static nitrogen atmosphere at 120 °C for 48 h. The reaction was then cooled to room temperature, diluted with 50 mL of CH_2Cl_2 and filtered on Celite. The organic phase was evaporated in vacuum and the solid crude reaction mixture was further purified by automatic flash chromatography on SiO_2 with a gradient of CH_2Cl_2 /Hexane as eluents to give the **(2-Th)$_3$TT** as a white solid (0.148 g, 33% Yield, R_f = 0.73 in CH_2Cl_2).

NMR data (9.4 T, DMSO-d$_6$, 298 K, δ, ppm) ^{1}H NMR 7.70 (dd, *J* = 5.1, 1.2 Hz, 1H), 7.62 (dd, *J* = 3.6, 1.2 Hz, 1H), 7.35 (s, 1H), 7.19 (dd, *J* = 5.1, 3.6 Hz, 1H).**^{13}C NMR** 136.60 (C), 130.11 (CH), 128.27 (CH), 128.25 (C), 127.61 (CH), 127.26 (CH), 120.70 (C) (Figures S7-S8).
MS (ESI-positive ion mode): *m/z*: 444.96 $[M+H]^+$ (Figure S9).

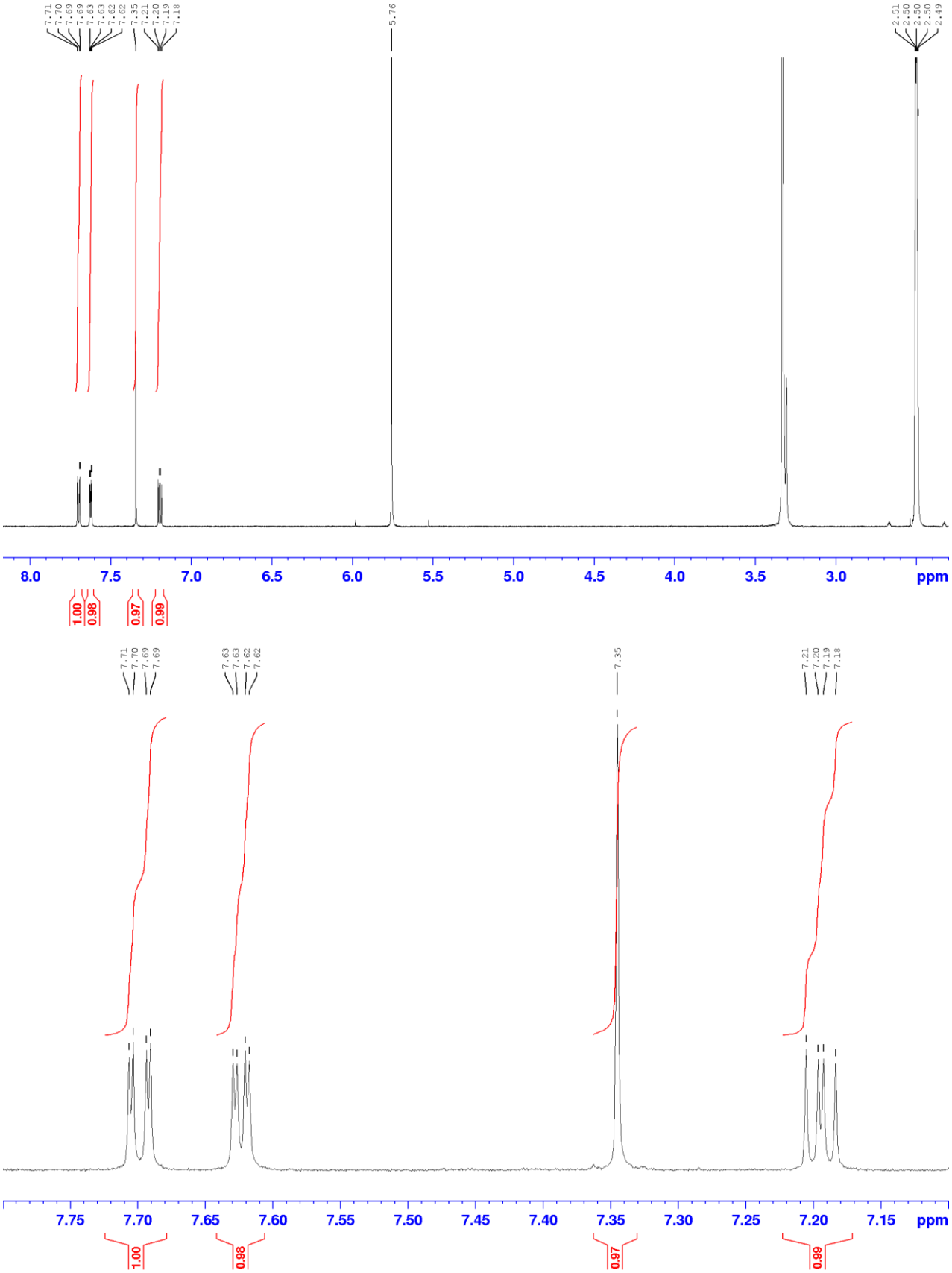

Figure S7: ^{1}H NMR spectrum of **(2-Th)$_3$TT** (400 MHz, DMSO-d$_6$, top) with expansion of aromatic region (bottom).

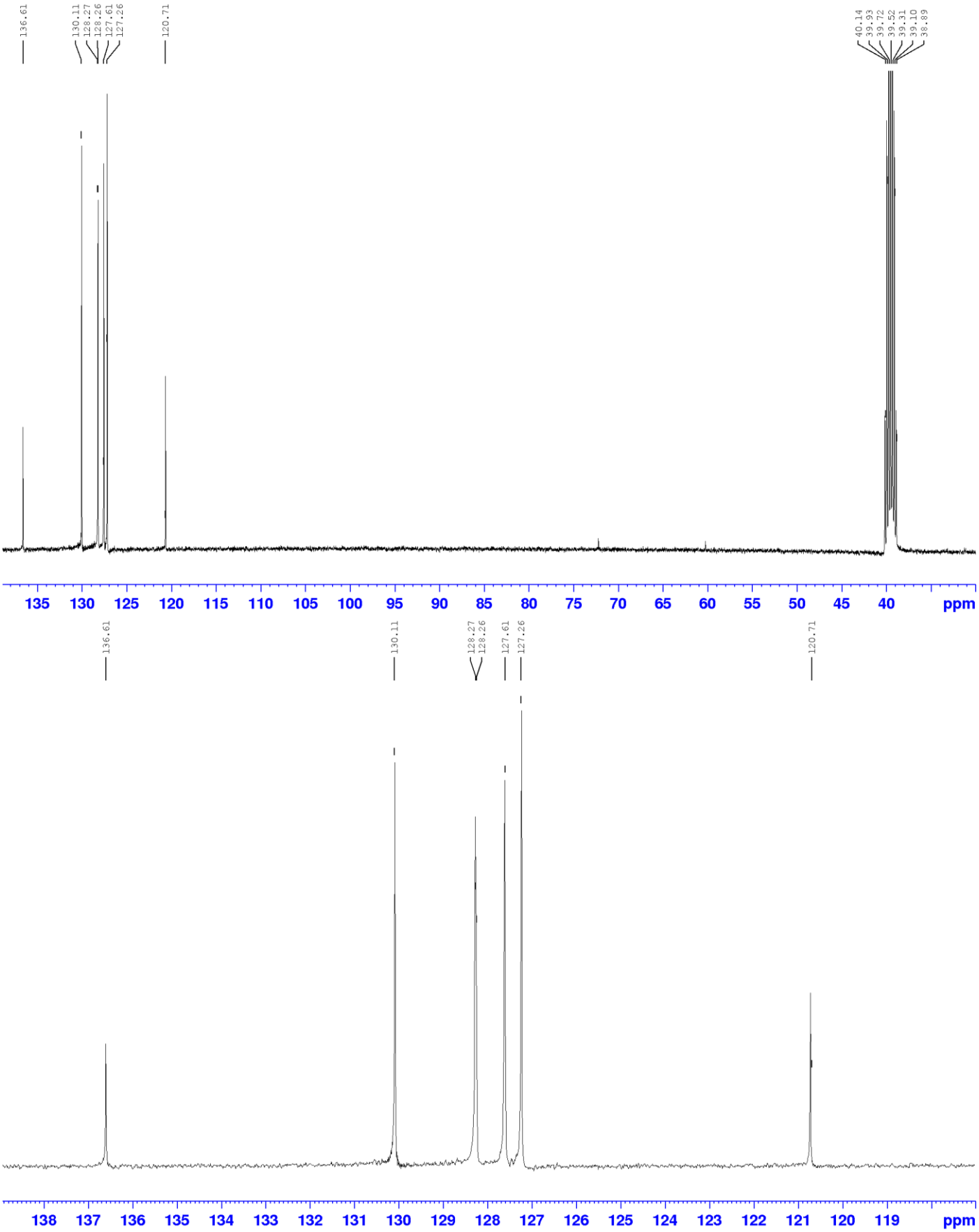

Figure S8: ^{13}C NMR spectrum of **(2-Th)$_3$TT** (100 MHz, DMSO-d$_6$, top) with expansion of aromatic region (bottom).

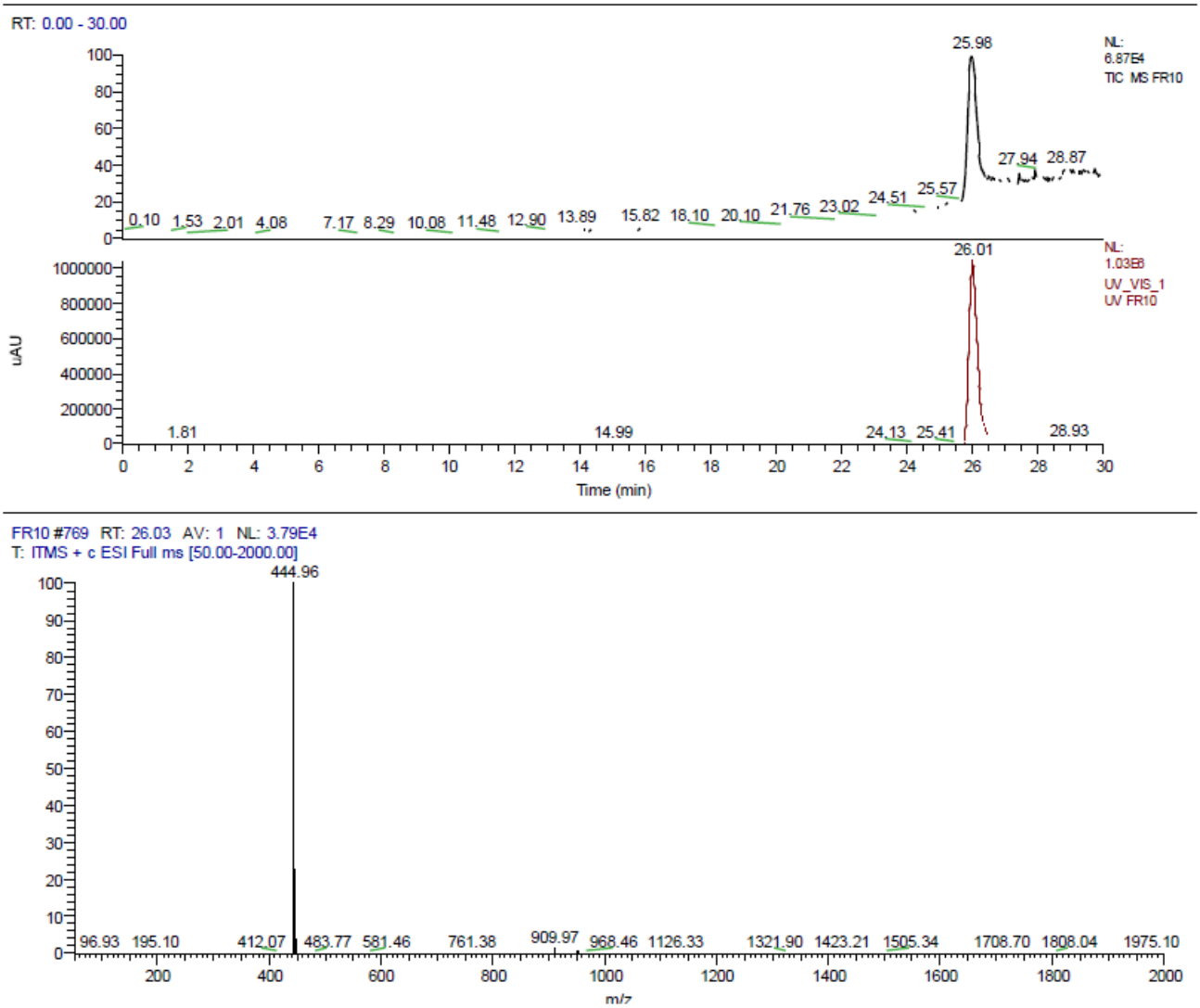

Figure S9: LC-MS profile of **(2-Th)$_3$TT**.

SI1.4 *Synthesis of 3-([2,2'-bithiophen]-5-yl)triimidazo[1,2-a:1',2'-c:1'',2''-e][1,3,5]triazine* **(2-biTh)TT**

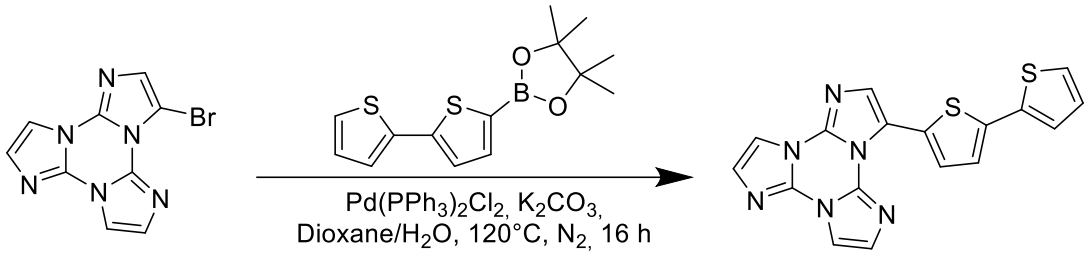

BrTT **(2-biTh)TT**

Scheme SI1.4 Synthetic path for the preparation of **(2-biTh)TT**

(2-biTh)TT was prepared by Suzuki-Miyaura cross coupling between **BrTT** and 2,2-bithiophene-5-boronic acid pinacol ester. In a typical reaction, **BrTT** (0.200 g; 0.722 mmol), 2,2 -bithiophene-5-boronic acid pinacol ester (0.232 g, 0.794 mmol), $Pd(PPh_3)_2Cl_2$ (0.051 g, 0.072 mmol), K_2CO_3 (0.998 g, 7.218 mmol), dioxane (8 mL) and H_2O (2 mL) were transferred inside a 100 mL Schlenk flask equipped with a magnetic stirrer. The system was heated under static nitrogen atmosphere at 120 °C for 48 h. The reaction was then cooled to room temperature, diluted with 50 mL of CH_2Cl_2 filtered on Büchner. The liquid phase was evaporated in vacuum and the crude was purified by flash chromatography on SiO_2 with CH_2Cl_2 /MeCN as eluents to give **(2-biTh)TT** product as a light green solid. Solid was further washed with MeCN getting a white compound (0.1517 g, 58 % Yield, Rf 0.30 in CH_2Cl_2/MeCN 10%).

NMR data (9.4 T, CD_2Cl_2, 298 K, δ, ppm) ^{1}**H NMR** 7.81 (t, *J* = 1.8 Hz, 2H), 7.69 (d, *J* = 3.8 Hz, 1H), 7.34 – 7.23 (m, 6H), 7.07 (dd, *J* = 5.1, 3.6 Hz, 1H). ^{13}**C NMR** 139.18 (C), 137.19 (C), 136.60 (C), 131.44 (CH), 129.67 (CH), 129.27 (CH), 129.08 (CH), 128.44 (CH), 127.39 (C), 125.47 (CH), 124.71 (CH), 124.33 (CH), 122.47 (C), 114.20 (C), 112.07 (CH), 111.75 (CH) (Figures S10-S11).

MS (ESI-positive ion mode): *m/z*: 363.23 $[M+H]^+$ (Figure S12).

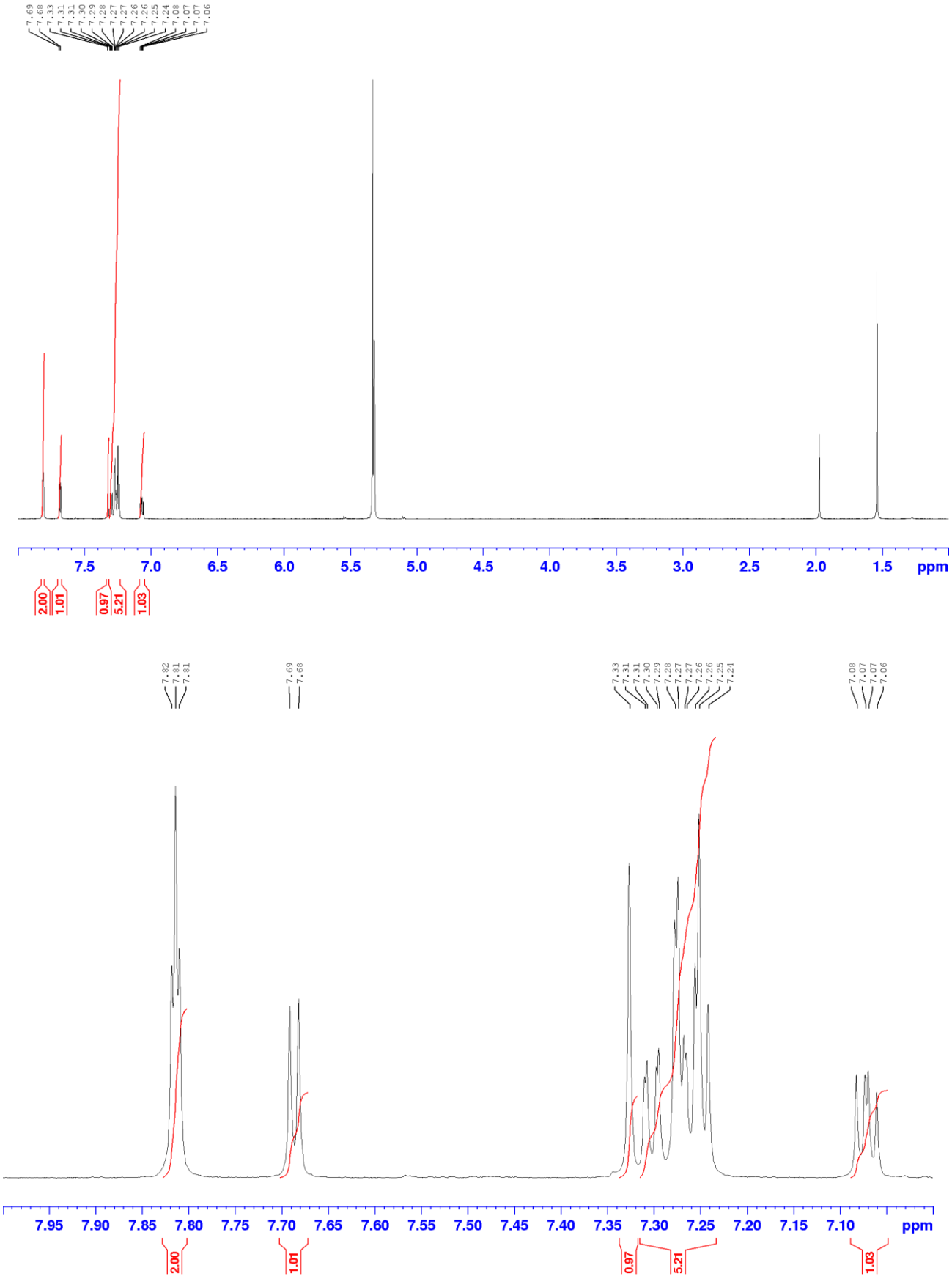

Figure S10: ^{1}H NMR spectrum of **(2-biTh)TT** (400 MHz, CD_2Cl_2, top) with expansion of aromatic region (bottom).

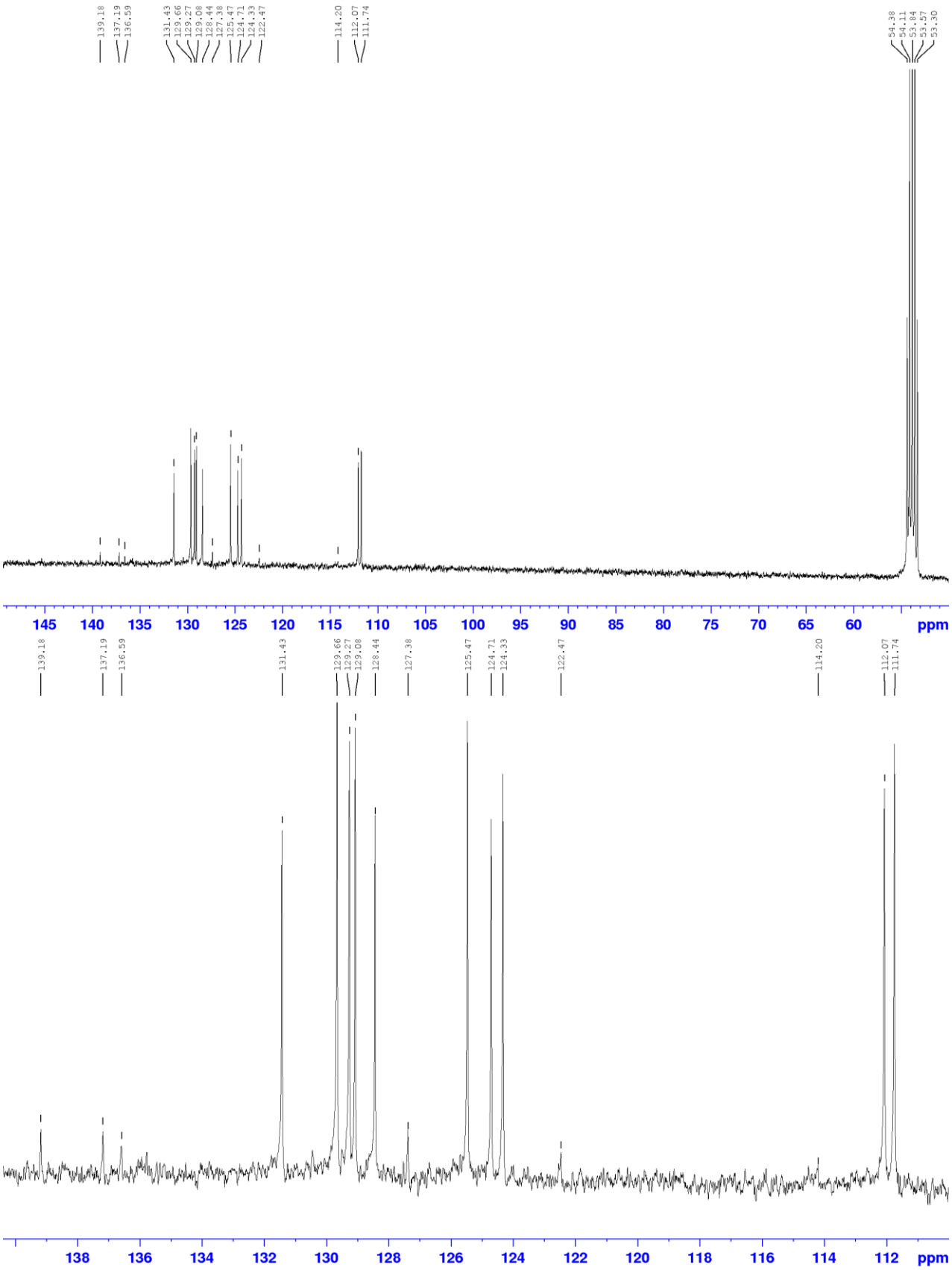

Figure S11: ^{13}C NMR spectrum of **(2-biTh)TT** (100 MHz, CD_2Cl_2, top) with expansion of aromatic region (bottom).

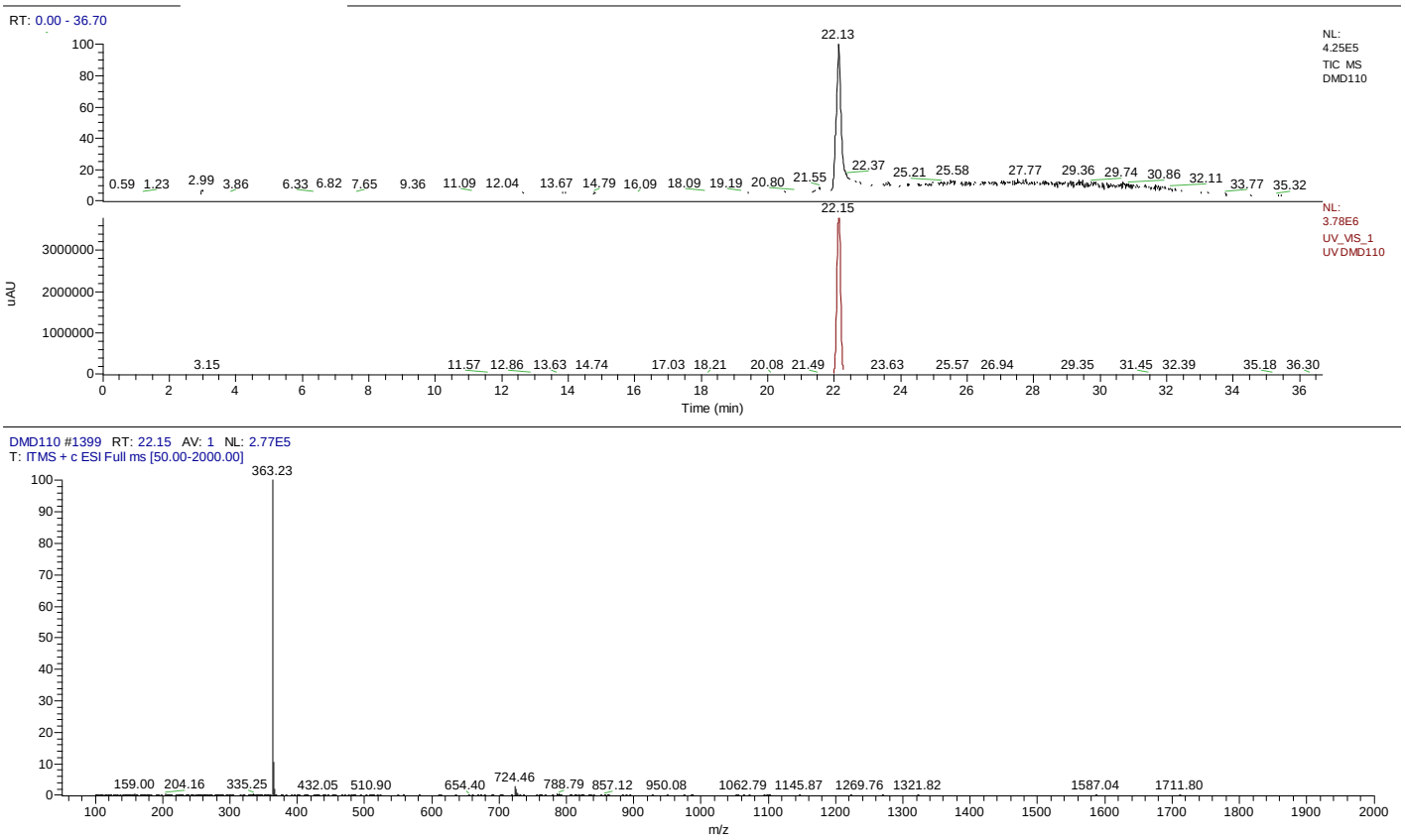

Figure S12: LC-MS profile of **(2-biTh)TT**.

SI1.5 *Synthesis of 3,7-di([2,2'-bithiophen]-5-yl)triimidazo[1,2-a:1',2'-c:1",2"-e][1,3,5]triazine* **(2-biTh)$_2$TT**

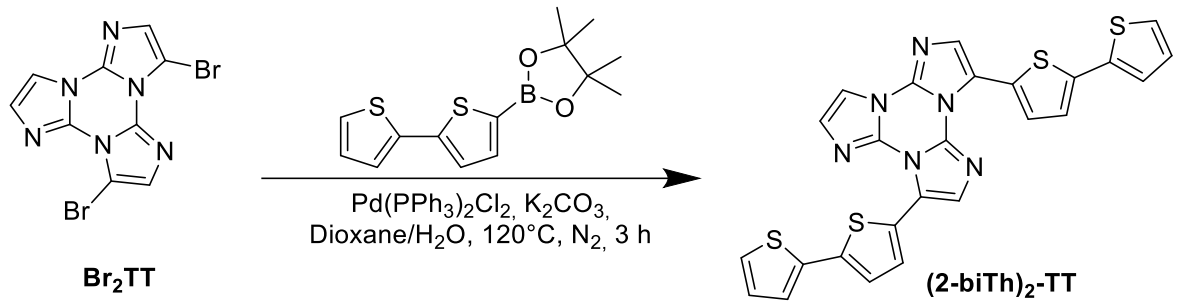

Scheme SI1.5 Synthetic path for the preparation of **(2-biTh)$_2$TT**

(2-biTh)$_2$TT was prepared by Suzuki-Miyaura cross coupling between **Br$_2$TT** and 2,2 -bithiophene-5-boronic acid pinacol ester. In a typical reaction, **Br$_2$TT** (0.100 g; 0.281 mmol), 2,2 -bithiophene-5-boronic acid pinacol ester (0.181 g, 0.618 mmol), Pd(PPh$_3$)$_2$Cl$_2$ (0.020 g, 0.028 mmol), K$_2$CO$_3$ (0.388 g, 2.809 mmol), 1,4-Dioxane (8 mL) and H$_2$O (2 mL) were transferred inside a 100 mL Schlenk flask equipped with a magnetic stirrer. The system was heated under static nitrogen atmosphere at 120 °C for 3 h. The reaction was then cooled to room temperature, diluted with 50 mL of water and filtered on Büchner and the solid recover and dried in vacuum. The crude was purified by flash chromatography on SiO$_2$ with DCM/ACN as eluents to give **(2-biTh)$_2$TT** product as a light green solid. (0.076 g, 51 % Yield, R$_f$ = 0.45 in DCM/ACN=96/4).
NMR data (9.4 T, CD$_2$Cl$_2$, 298 K, δ, ppm) ^{1}H NMR 7.84 (d, *J* = 1.6 Hz, 1H), 7.65 (m, 2H), 7.34 – 7.22 (m, 9H), 7.10 – 7.05 (m, 2H). **^{13}C NMR** 139.18 (C), 137.04 (C), 136.51 (C), 136.33 (C), 135.65 (C), 131.52 (CH), 131.42 (CH), 130.53(CH), 129.58 (CH), 129.26 (CH), 129.08 (CH), 128.98 (CH), 128.38 (CH), 127.21 (C), 127.09 (C), 125.40 (CH), 124.60 (CH), 124.16 (CH), 122.33 (C), 121.86 (C), 111.69 (C) (Figures S13-S14).
MS (ESI-positive ion mode): *m/z*: 527.23 $[M+H]^+$ (Figure S15).

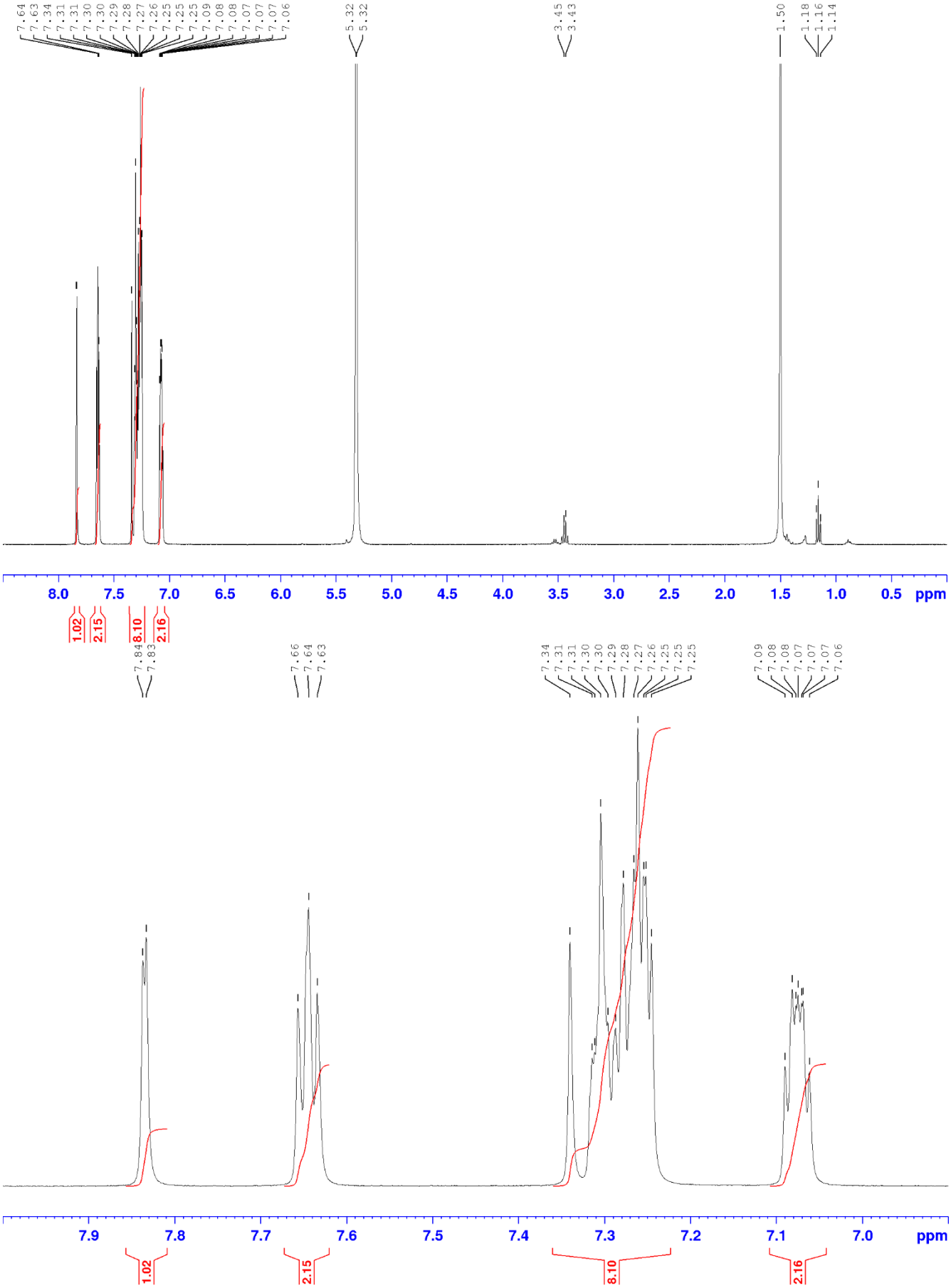

Figure S13: ^{1}H NMR spectrum of **(2-biTh)$_2$TT** (400 MHz, CD_2Cl_2, top) with expansion of aromatic region (bottom).

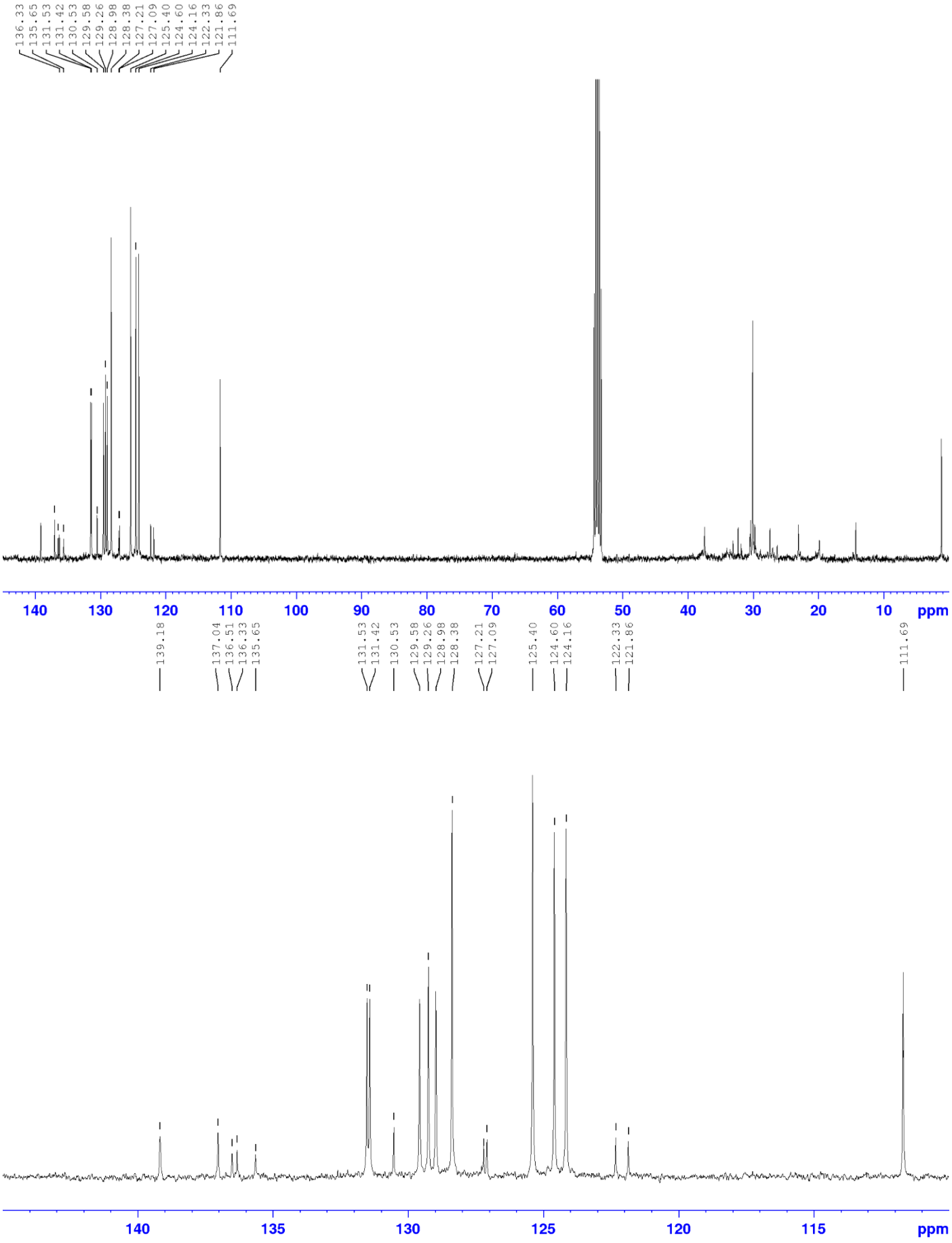

Figure S14: ^{13}C NMR spectrum of **(2-biTh)$_2$TT** (100 MHz, CD_2Cl_2, top) with expansion of aromatic region (bottom).

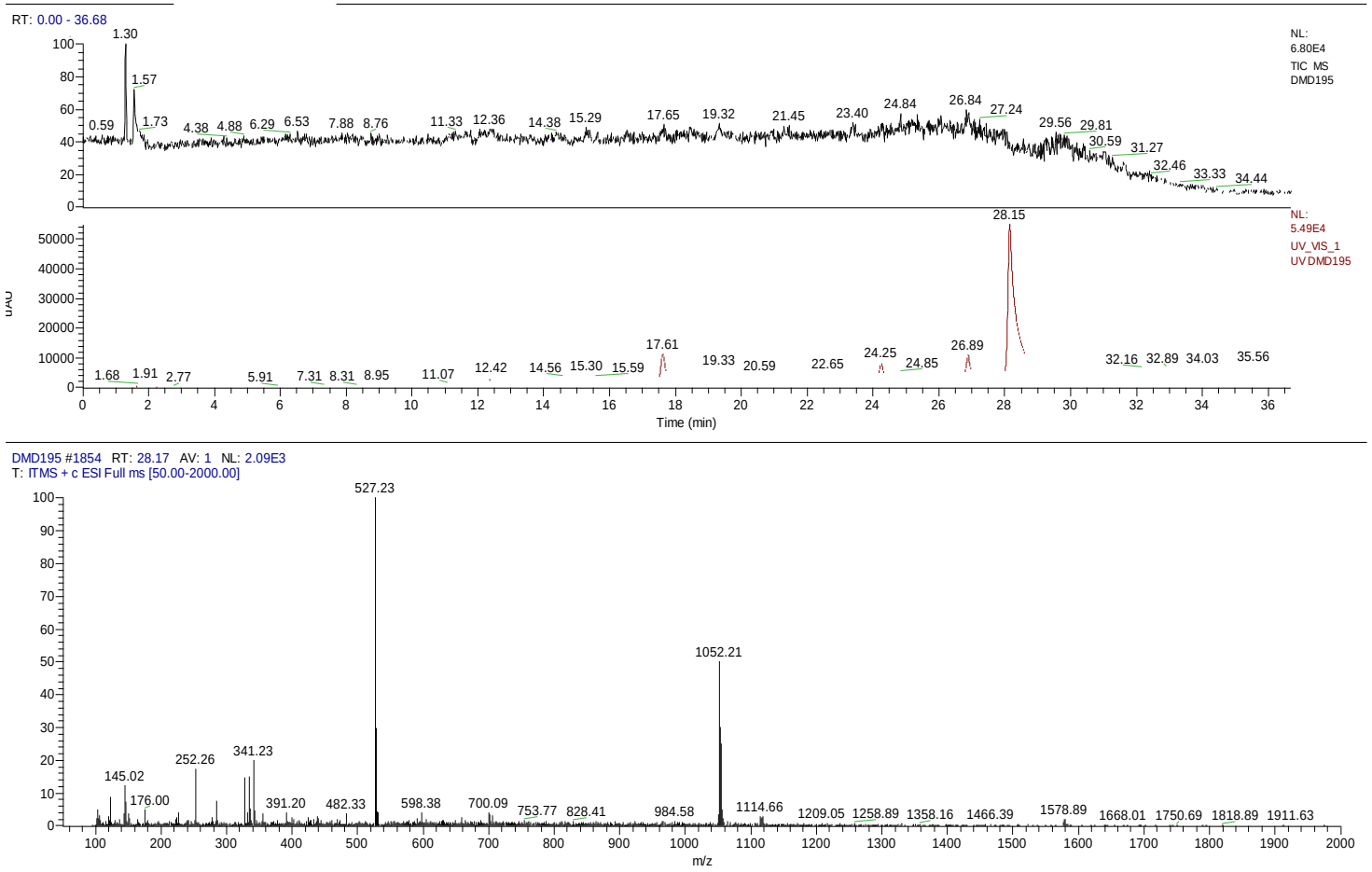

Figure S15: LC-MS profile of **(2-biTh)$_2$TT**.

SI1.6 *Synthesis of 3,7,11-tri([2,2'-bithiophen]-5-yl)triimidazo[1,2-a:1',2'-c:1'',2''-e][1,3,5]triazine* **(2-biTh)$_3$TT**

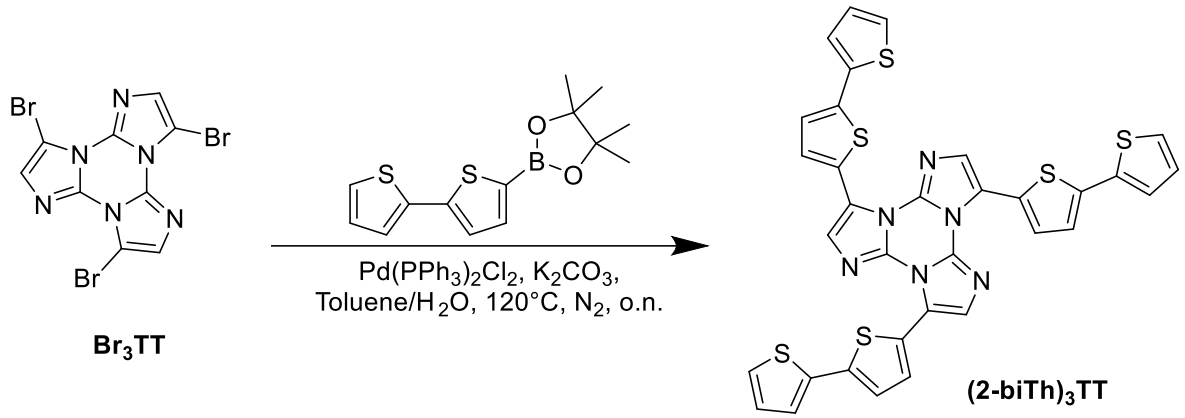

Scheme SI Synthetic path for the preparation of **(2-biTh)$_3$TT**

(2-biTh)$_3$TT was prepared by Suzuki-Miyaura cross coupling between **Br$_3$TT** and 2,2 -bithiophene-5-boronic acid pinacol ester. In a typical reaction, **Br$_3$TT** (0.0580 g; 0.135 mmol), 2,2 -bithiophene-5-boronic acid pinacol ester (0.123 g, 0.419 mmol), $Pd(PPh_3)_2Cl_2$ (0.009 g, 0.013 mmol), K_2CO_3 (0.186 g, 1.352 mmol), Toluene (9 mL) and H_2O (1 mL) were transferred inside a 100 mL Schlenk flask equipped with a magnetic stirrer. The system was heated under static nitrogen atmosphere at 120 °C overnight. The reaction was then cooled to room temperature, filtered on Büchner and the liquids dried under vacuum. The crude was purified by flash chromatography on SiO_2 with PE/DCM as eluents to give **(2-biTh)$_3$TT** product as a yellow solid. (0.041 g, 43 % Yield, R_f = 0.51 in PE/DCM=3/7).

NMR data (9.4 T, $CDCl_3$, 298 K, δ, ppm) ^{1}H NMR 7.61 (d, J = 3.8 Hz, 3H), 7.32 (s, 3H), 7.29 – 7.25 (m), 7.07 – 7.05 (dd, J_1 = 5.0 Hz, J_2 = 3.6 Hz, 3H).

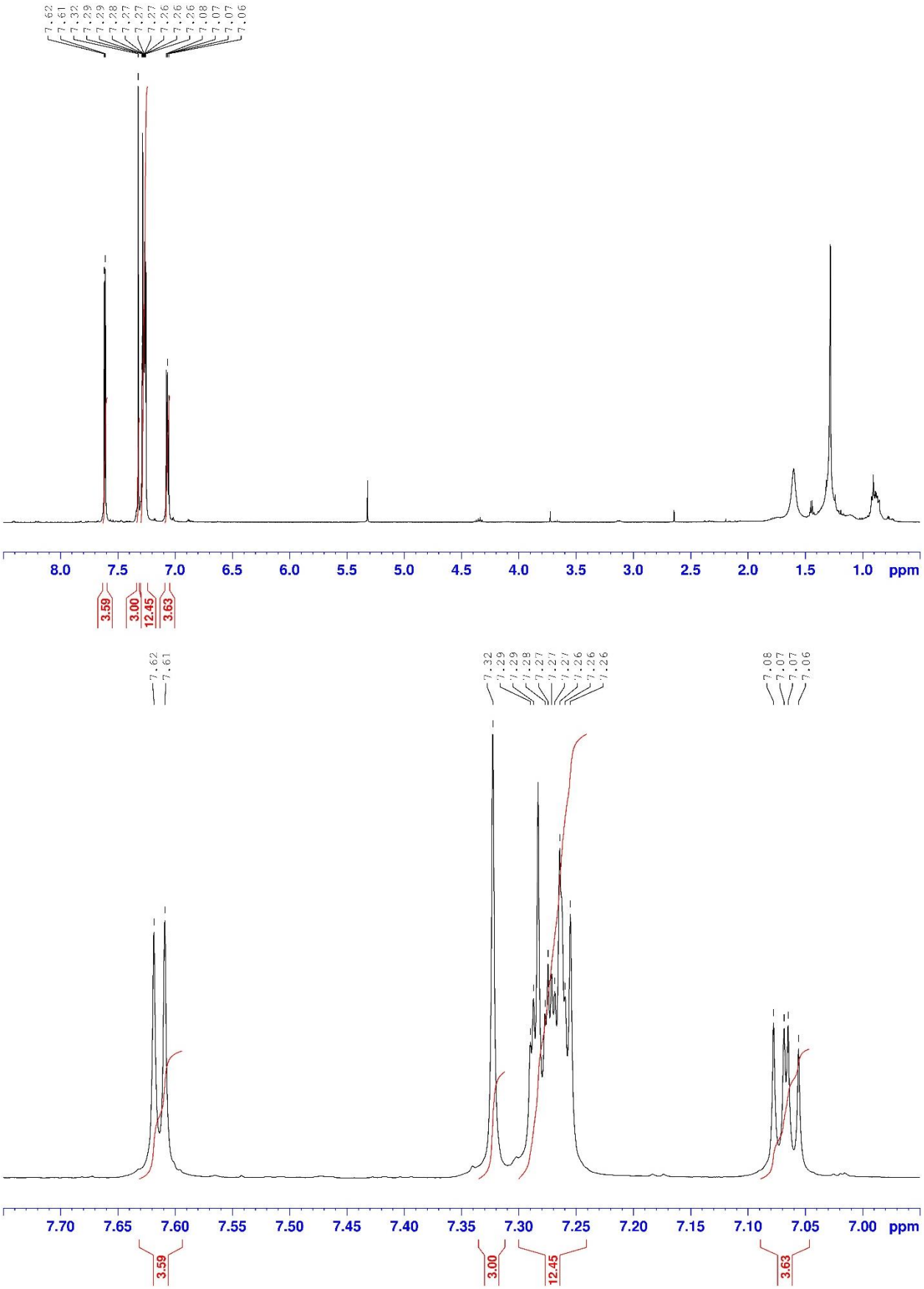

Figure S16: ^{1}H NMR spectrum of **(2-biTh)$_3$TT** (400 MHz, $CDCl_3$, top) with expansion of aromatic region (bottom).

SI1.7 Product characterization

^{1}H and ^{13}C NMR spectra were recorded on a Bruker AVANCE-400 instrument (400 MHz). Chemical shifts are reported in parts per million (ppm) and are referenced to the residual solvent peak (DMSO, ^{1}H: δ=2.50 ppm, ^{13}C: δ=39.5 ppm; CD_2Cl_2, ^{1}H: δ=5.32 ppm, ^{13}C: δ=54.0 ppm). Mass spectra were recorded on a Thermo Fisher LCQ Fleet Ion Trap Mass Spectrometer equipped with UltiMate™ 3000 HPLC system.

UV-Visible spectra were collected by UV-3600i Plus UV-VIS-NIR Spectrophotometer (Shimadzu Italia S.r.l., Milan, Italy).
Photoluminescence quantum yields have been measured using a C11347 Quantaurus–Absolute Photoluminescence Quantum Yield Spectrometer (Hamamatsu Photonics K.K), equipped with a 150 W Xenon lamp, an integrating sphere and a multichannel detector. Steady state emission and excitation spectra and photoluminescence lifetimes have been obtained using a FLS 980 (Edinburgh Instrument Ltd) spectrofluorimeter. The steady state measurements have been recorded by a 450 W Xenon arc lamp. Photoluminescence lifetime measurements have been performed using a EPLED-300 (Edinburgh Instrument Ltd) and microsecond flash Xe-lamp (60W, 0.1÷100 Hz) with data acquisition devices time correlated single-photon counting (TCSPC) and multi-channel scaling (MCS) methods, respectively. Average lifetimes are obtained as $\tau_{av} = \frac{\sum A_i \tau_i^2}{\sum A_i \tau_i}$ from bi-exponential or three-exponential fits.

SI2. Key parameters concerning the TT derivatives estimated by DFT computations

Density functional theory DFT and time-dependent density functional theory TDDFT calculations on all the investigated molecules were performed in vacuo using the 6-311++G(d,p) basis set. Differently from previous calculations carried out on **TT** itself and other **TT** derivatives, for which the ωB97X functional was used, we adopted here the PBE0 functional [S1]. In fact, the latter functional has been widely demonstrated to reproduce with high accuracy, in a quantitative way, the ground and excited state properties of isolated molecules [S2], becoming one of the elective choices for DFT investigations on systems in solution. On the other hand, the ωB97X functional, while providing slightly blue-shifted excitation energies, allows to correctly describe also intermolecular interactions, such as π-π stacking interactions, which are crucial for interpreting the emissive properties of **TT** derivatives in solid state. Geometry optimization of all compounds have been performed starting from the respective X-ray geometries, when available, or from the X-ray geometry of analogue derivatives after the required substitutions. All calculations have been performed with Gaussian 16 program (Revision A.03) [S3].

Detailed results are reported in Table SI2.1 (following page)

[S1] C. Adamo, V. Barone, Toward reliable density functional methods without adjustable parameters: The PBE0 model. J. Chem. Phys. 110 (1999) 6158−6170.

[S2] S. Di Grande, I. Ciofini, C. Adamo, M. Pagliai, G. Cardini, Absorption Spectra of Flexible Fluorescent Probes by a Combined Computational Approach: Molecular Dynamics Simulations and Time-Dependent Density Functional Theory, J. Phys. Chem. A 126 (2022) 8809-8817.

[S3] M. J. Frisch, G. W. Trucks, H. B. Schlegel, G. E. Scuseria, M. A. Robb, J. R. Cheeseman et al. Gaussian 16, Revision A.03; Gaussian, Inc.: Wallingford, CT, USA, 2016.

SI2. Key parameters concerning the TT derivatives estimated by DFT computations

Table SI2.1 HOMO and LUMO energies (eV), HOMO-LUMO energy gap (ΔE_{H-L}, eV), dipole moments (D) of the ground (μ_0) and S_i excited (μ_{Si},) states, excitation energies (E_{exc}, nm) and main contributions to the transitions with associated weights.[a]

compound	E_{HOMO}	E_{LUMO}	ΔE_{H-L}	μ_0	μ_{Si}	E_{exc}, f	Main contributions, weight
TT	-6.83	-0.80	6.03	0.0	0.0 0.0 1.97 1.97	S_1 252, 0.0000 S_2 245, 0.0000 S_3 226, 0.3036 S_4 226, 0.3037	H-1→L+1, 47%; H→L, 47% H-1→L, 47%; H→L+1, 47% H-1→L, 39%; H→L+1, 39% H-1→L+1, 39%; H→L, 39%
(2-Py)TT	-6.41	-1.47	4.94	2.03	3.12	S_1 291, 0.4652	H→L, 94%
(4-Py)TT	-6.76	-1.58	5.18	2.52	7.21	S_1 278, 0.3456	H→L, 90%
(4-Py)$_2$TT	-6.84	-1.76	5.08	2.42	4.53 6.67 3.67	S_1 283, 0.0696 S_2 282, 0.1363 S_3 275, 0.4745	H-1→L, 67% H→L, 84% H→L+1, 46%; H-1→L, 14%
(4-Py)$_3$TT	-6.95	-1.85	5.10	0.06	0.65 0.28 0.89 0.50	S_1 291, 0.0039 S_2 283, 0.0031 S_3 277, 0.5671 S_4 277, 0.5802	H→L, 52%; H-1→L+1, 39% H-1→L, 47%; H→L+1, 44% H-1→L, 34%; H→L+1, 34% H-1→L+1, 40%; H→L, 28%
(2-Th)Me$_2$Im	-5.90	-0.87	5.03	4.12	5.73	S_1 286, 0.3192	H→L, 97%
(2-Th)TT	-6.17	-1.31	4.86	0.84	0.97	S_1 295, 0.4467	H→L, 97%
(2-Th)$_2$TT [b]	-6.14	-1.39	4.75	1.05	3.66 3.73	S_1 302, 0.1649 S_2 300, 0.2600	H-1→L, 73% H→L, 82%
(2-Th)$_3$TT [b]	-6.16	-1.38	4.78	1.12	1.15 1.14 2.91 2.92	S_1 311, 0.0000 S_2 300, 0.0005 S_3 298, 0.7187 S_4 298, 0.7182	H-1→L, 48%; H→L+1, 48% H-1→L+1, 48%; H→L, 49% H-1→L+1, 33%; H→L, 32% H-1→L, 33%; H→L+1, 33%
(2-biTh)TT	-5.78	-1.75	4.03	0.48	0.39	S_1 357, 0.8772	H→L, 99%
(2-biTh)$_2$TT	-5.79	-1.81	3.98	0.67	1.33	S_1 365, 1.3297	H-1→L, 77%; H→L+1, 21%
(2-biTh)$_3$TT	-5.80	-1.80	4.00	0.70	1.34	S_1 365, 1.3394	H-2→L, 40%; H→L, 25%; H-1→L+1, 25%

[a] Geometry optimization and TDDFT calculations performed *in vacuo* at PBE0/6-311++G(d,p) level of theory.
[b] All thiophene S atoms on the same side with respect to the **TT** plane.

SI3. Supplementary Absorption/Emission/Lifetime spectra

SI3.1 Absorption spectrum of parent **TT** in CH_2Cl_2

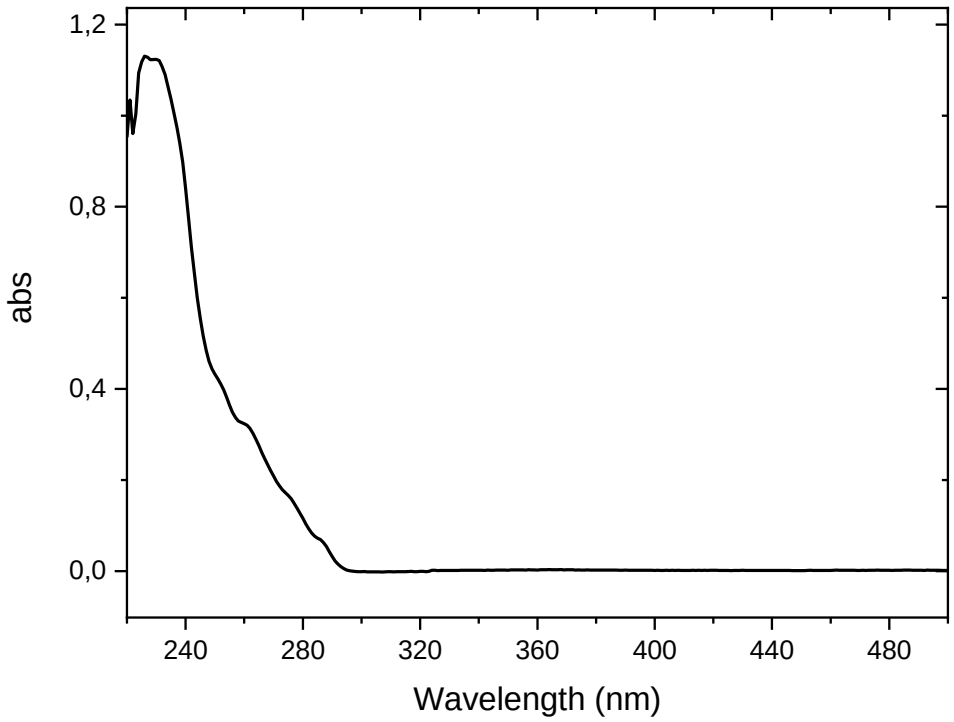

Figure S17: Absorption spectrum of **TT** in CH_2Cl_2 ($2.5x10^{-5}$M) at 298 K.

SI3.2 Absorption and emission spectra of **(4-Py)$_n$TT** in CH_2Cl_2

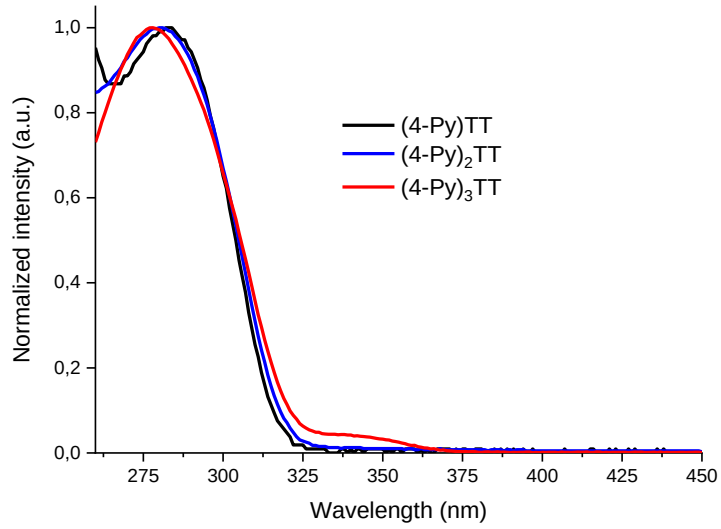

Figure S18: Normalized absorption spectra of 10^{-5} M CH_2Cl_2 solutions of **(4-Py)$_n$TT** at 298 K.

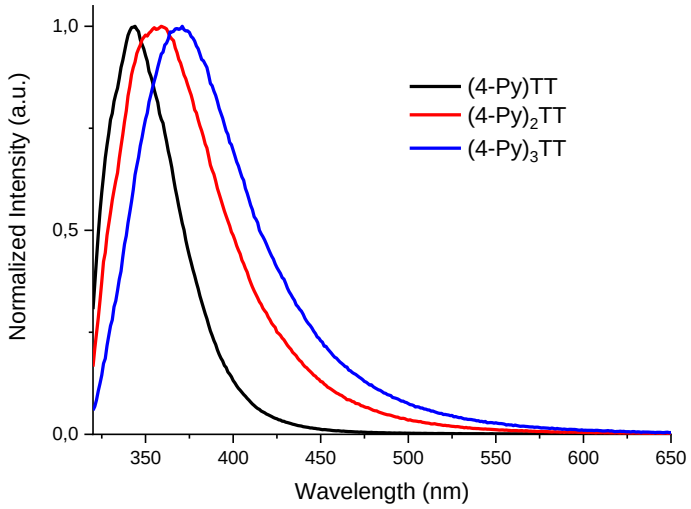

Figure S19: Normalized emission spectra of 10^{-5} M CH_2Cl_2 solutions of **(4-Py)$_n$TT** at 298 K (λ_{exc} = 300 nm).

SI3.3 Absorption and emission spectra of **(2-Th)$_n$TT** and **(2-biTh)$_n$TT** in CH_2Cl_2

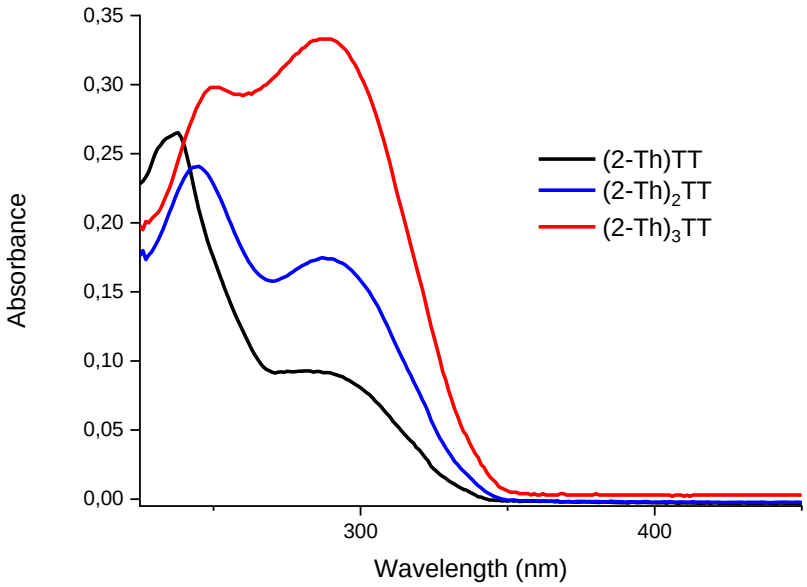

Figure S20: Absorption spectra of 10^{-5} M CH_2Cl_2 solutions of **(2-Th)$_n$TT** at 298 K.

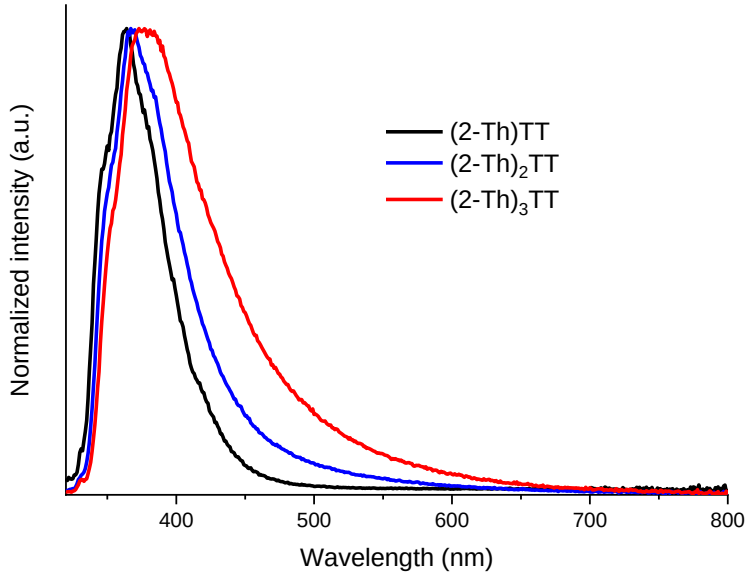

Figure S21: Normalized emission spectra of 10^{-5} M CH_2Cl_2 solutions of **(2-Th)$_n$TT** at 298 K (λ_{exc} = 300 nm).

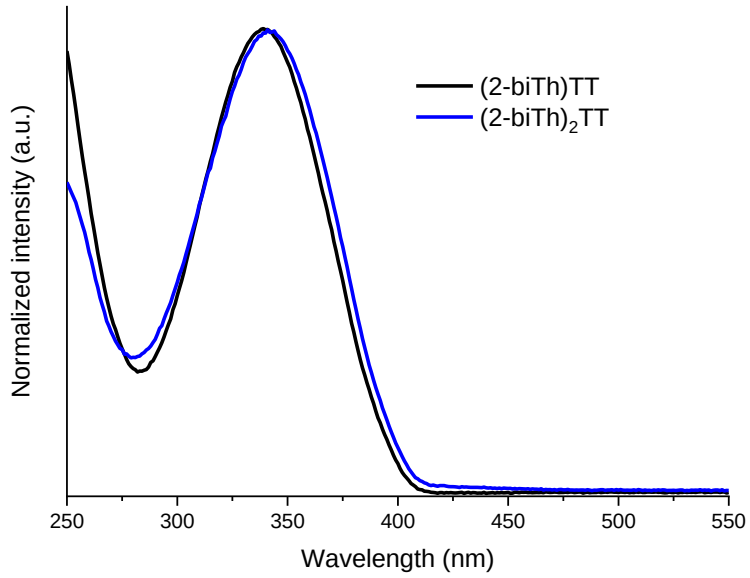

Figure S22: Normalized absorption spectra of 10^{-5} M CH_2Cl_2 solutions of **(2-biTh)TT and (2-biTh)$_3$TT** at 298 K.

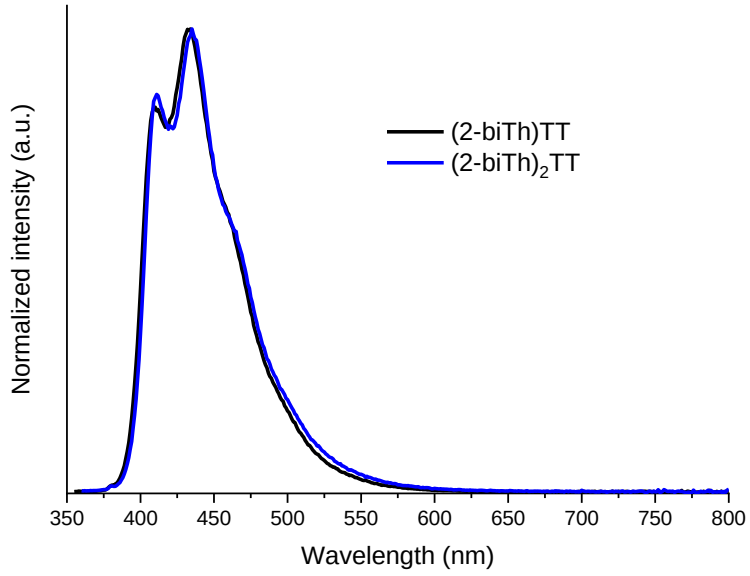

Figure S23: Normalized emission spectra of 10^{-5} M CH_2Cl_2 solutions of **(2-biTh)$_n$TT** at 298 K (λ_{exc} = 340 nm).

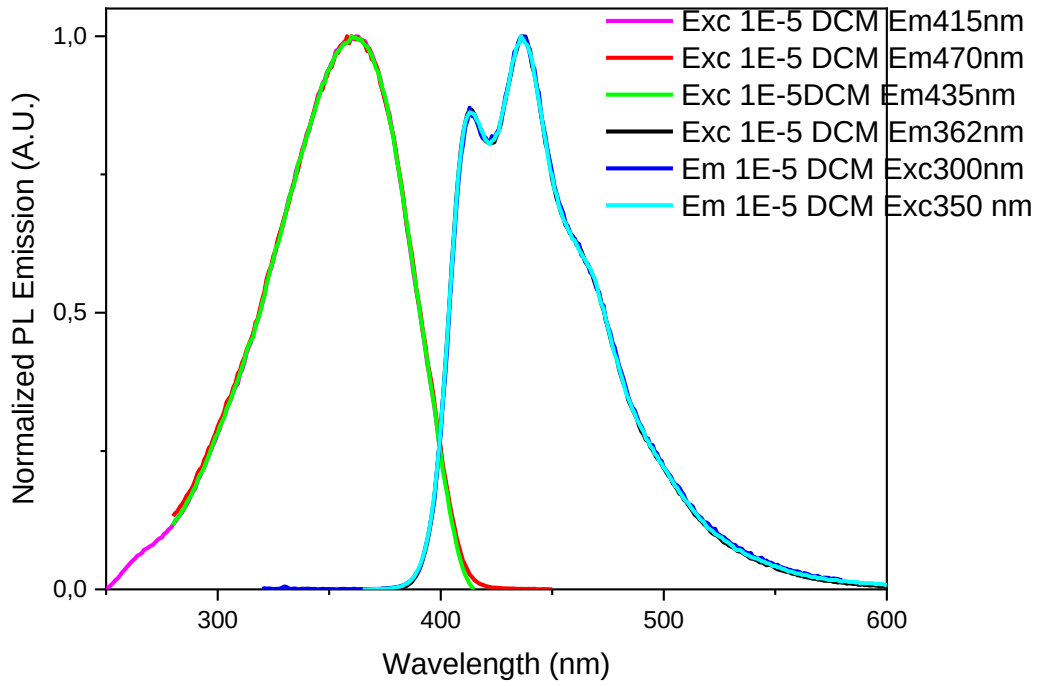

Figure S24: Normalized absorption and emission spectra of 10^{-5} M CH_2Cl_2 solutions of **(2-biTh)$_3$TT** at 298 K.

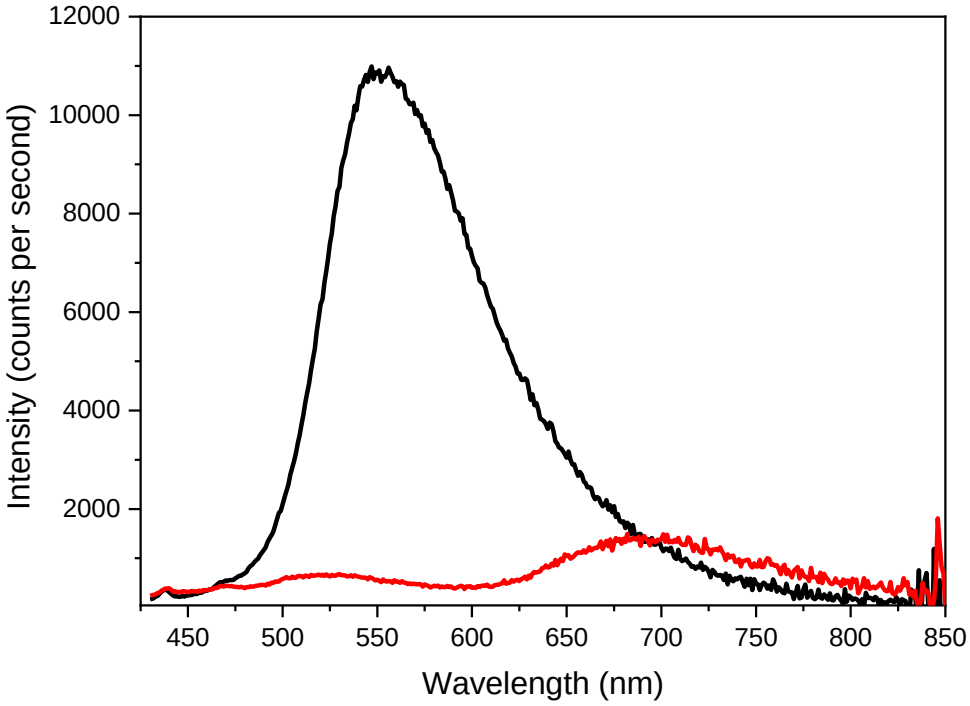

Figure S25: Emission spectra (λ_{exc} = 410 nm, 298 K) of **[(2-biTh)TT]$_n$** film: neutral (black line) and after polarization at 1.2V for 3 minutes (red line).

SI3.4 Lifetime spectra

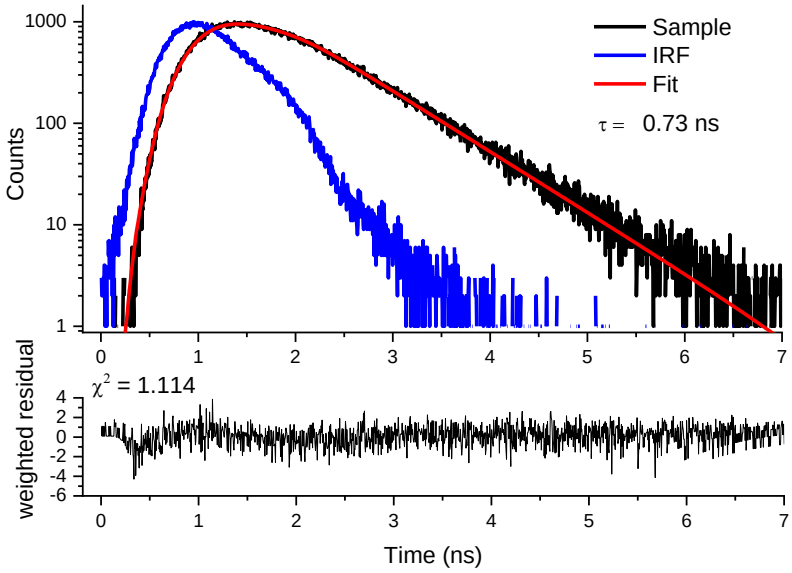

Figure S26: Lifetime measurement (λ_{exc} = 300 nm, λ_{em} = 343 nm) of **(4-Py)TT** in CH_2Cl_2 $1 \cdot 10^{-5}$ M, 298 K.

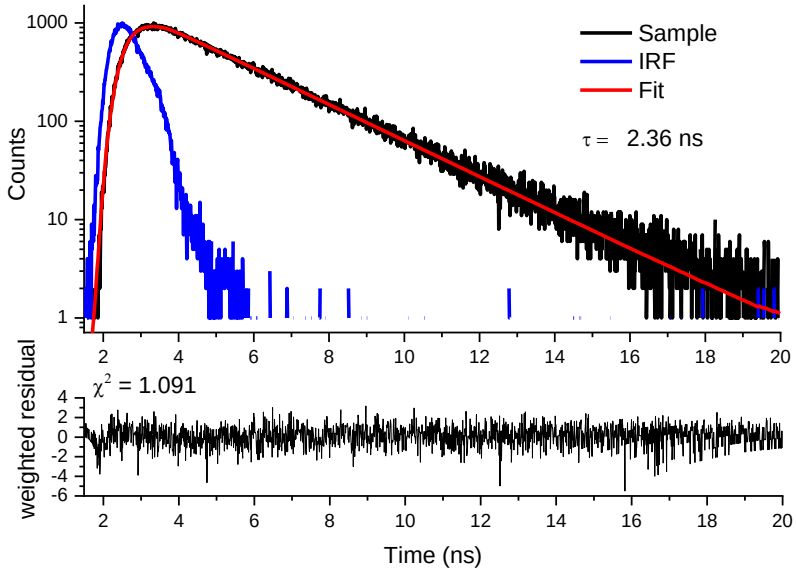

Figure S27: Lifetime measurement (λ_{exc} = 300 nm, λ_{em} = 357 nm) of **$(4\text{-Py})_2$TT** in CH_2Cl_2 $1 \cdot 10^{-5}$ M, 298 K.

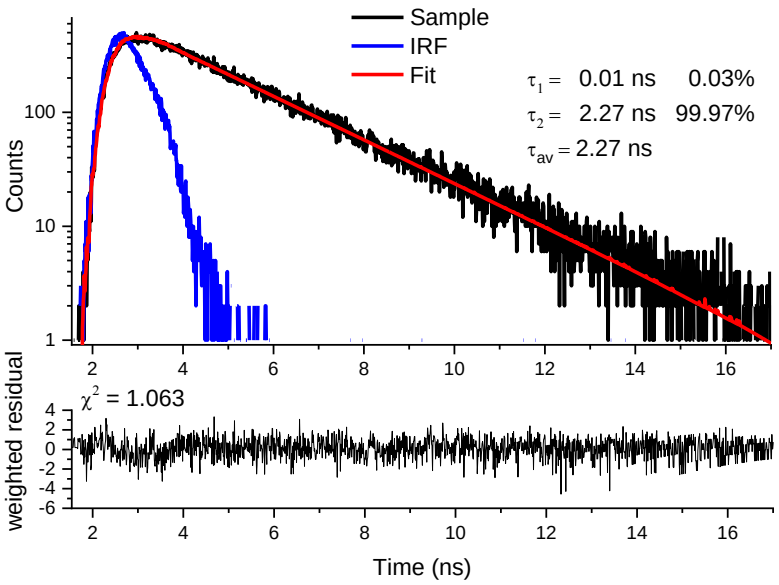

Figure S28: Lifetime measurement (λ_{exc} = 300 nm, λ_{em} = 370 nm) of **(4-Py)$_3$TT** in CH_2Cl_2 1·10^{-5} M, 298 K.

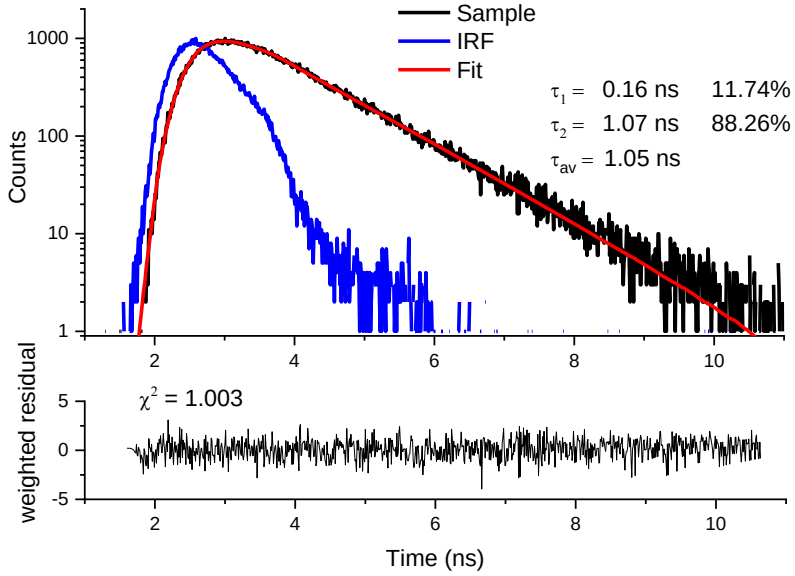

Figure S29: Lifetime measurement (λ_{exc} =300 nm, λ_{em} = 368 nm) of **(2-Th)$_2$TT** in CH_2Cl_2 1·10^{-5} M, 298 K.

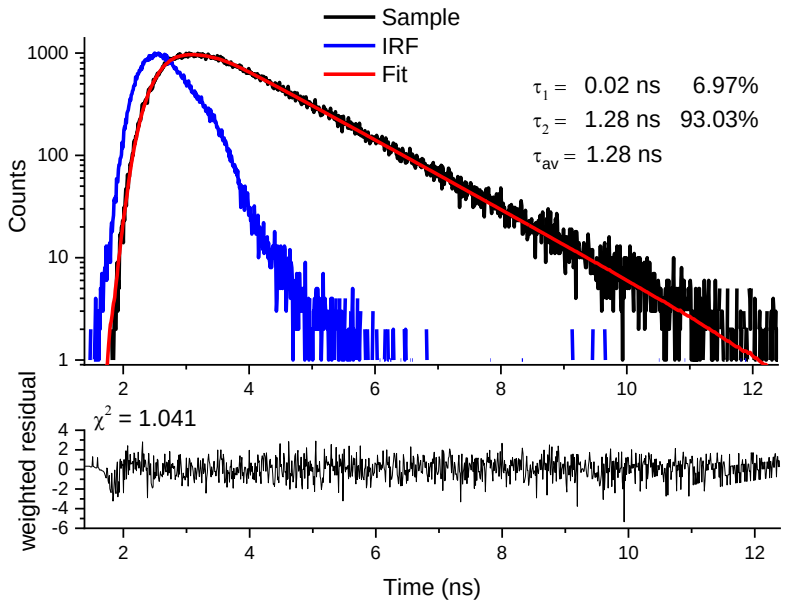

Figure S30: Lifetime measurement (λ_{exc} =300 nm, λ_{em} = 379 nm) of **(2-Th)$_3$TT** in CH_2Cl_2 $1\cdot10^{-5}$ M, 298 K.

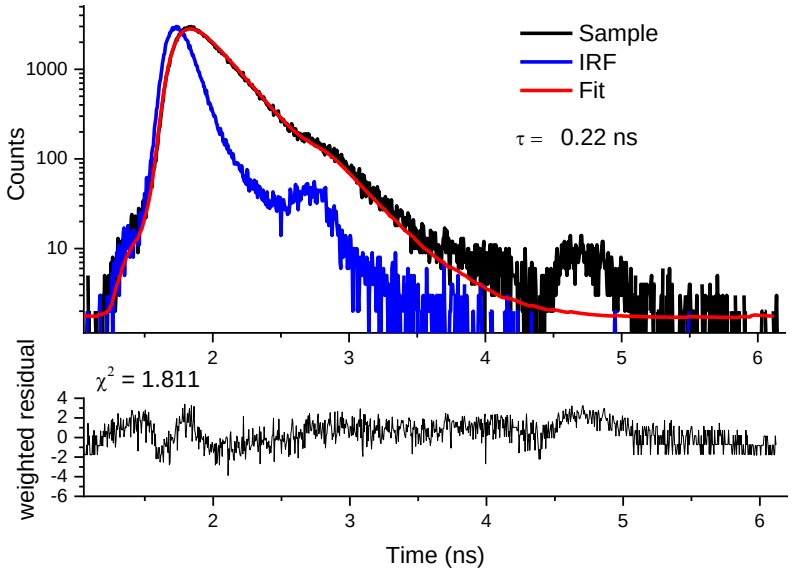

.

Figure S31: Lifetime measurement (λ_{exc}=374 nm, λ_{em} =433 nm) of **(2-biTh)TT** in CH_2Cl_2 $1\cdot10^{-5}$ M, 298 K.

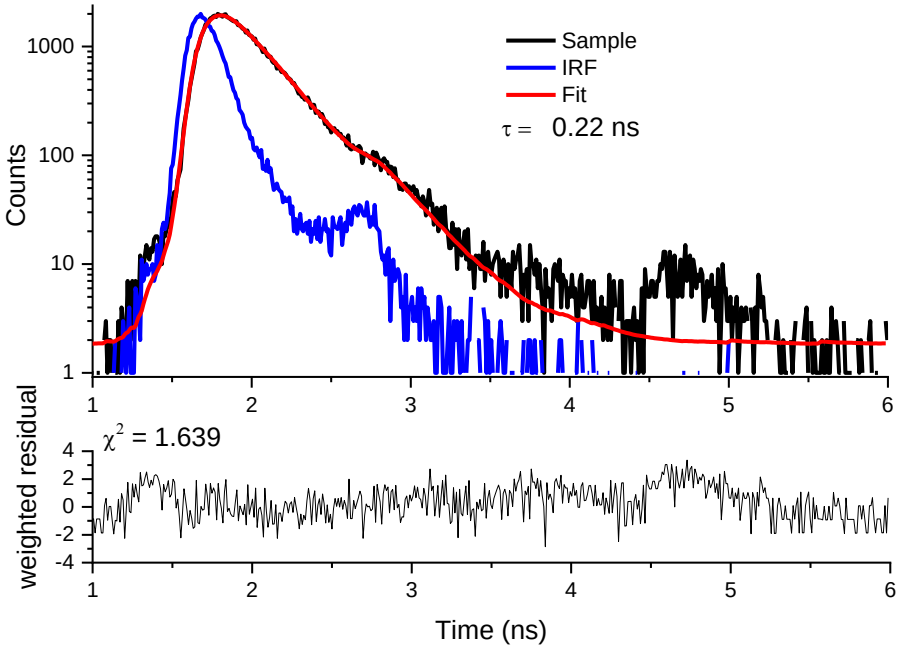

Figure S32: Lifetime measurement (λ_{exc}=374 nm, λ_{em}=433 nm) of **(2-biTh)$_2$TT** in CH_2Cl_2 $1\cdot10^{-5}$ M, 298 K.

SI4. Supplementary Electrochemical/Spectroelectrochemical data

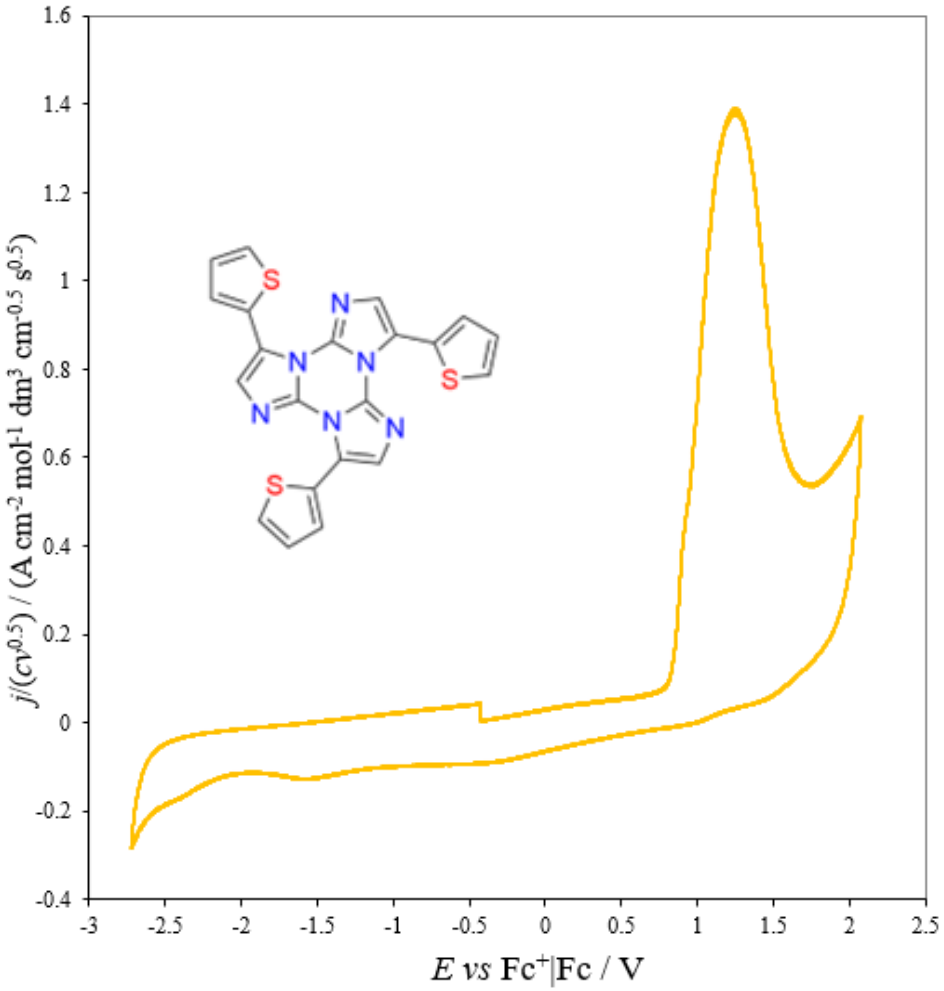

Figure S33. Normalized CV pattern for **(2-Th)$_3$TT** at 0.2 V/s in CH_2Cl_2 + 0.1 M $TBAPF_6$.

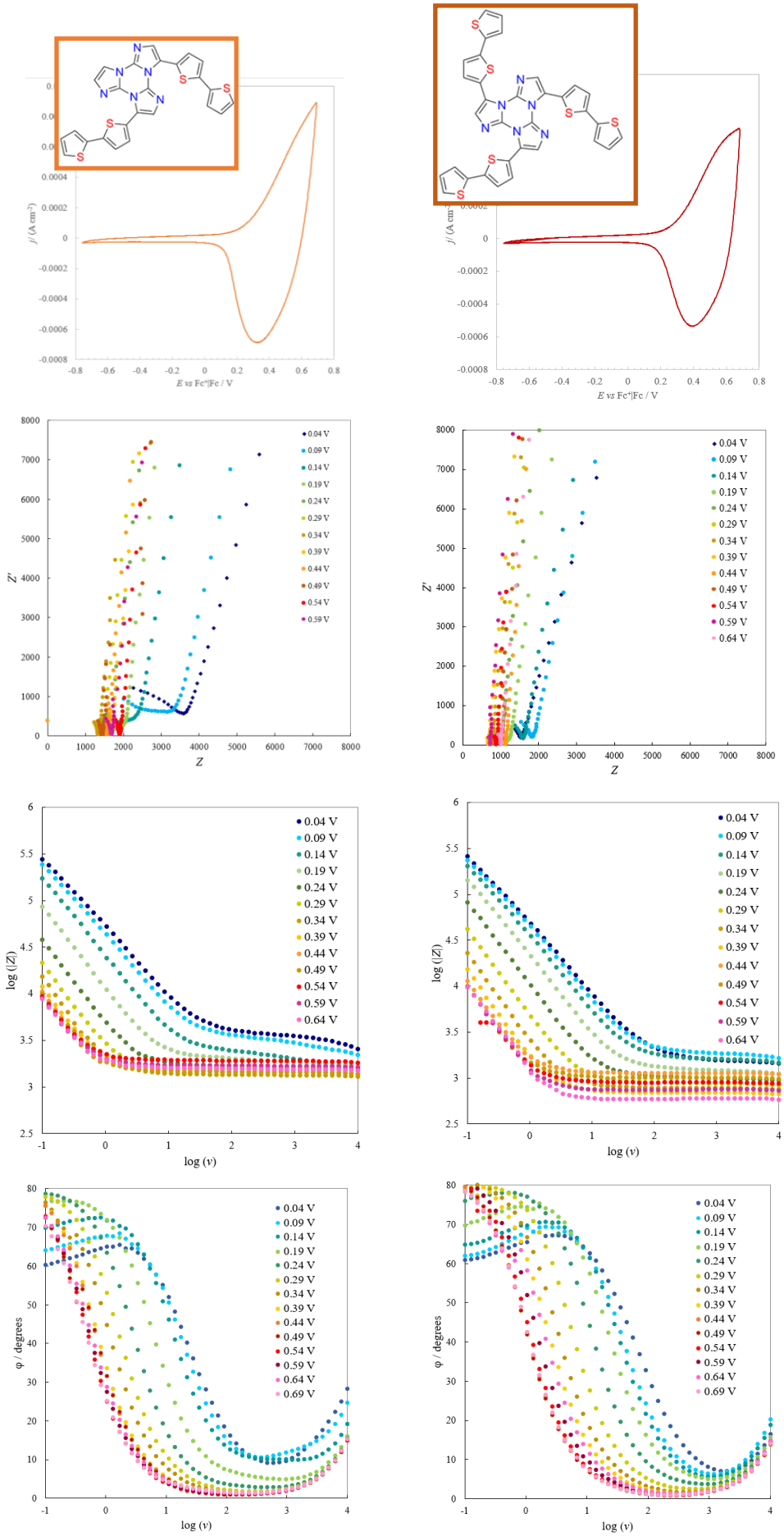

Figure S34. A comparison of EIS features at different potentials for (left) a **[(2-BiTh)$_2$TT]$_n$** film and (right) a **[(2-BiTh)$_3$TT]$_n$** film, both of them electrodeposited on a GC electrode in CH_2Cl_2 with 0.1 M $TBAPF_6$, by 12 potential cycles at 0.2 V/s scan rate followed by some stability cycles in monomer free solution. From top to bottom in each column: stability cycle; Nyquist diagram; Bode modulus diagram; Bode phase diagram.

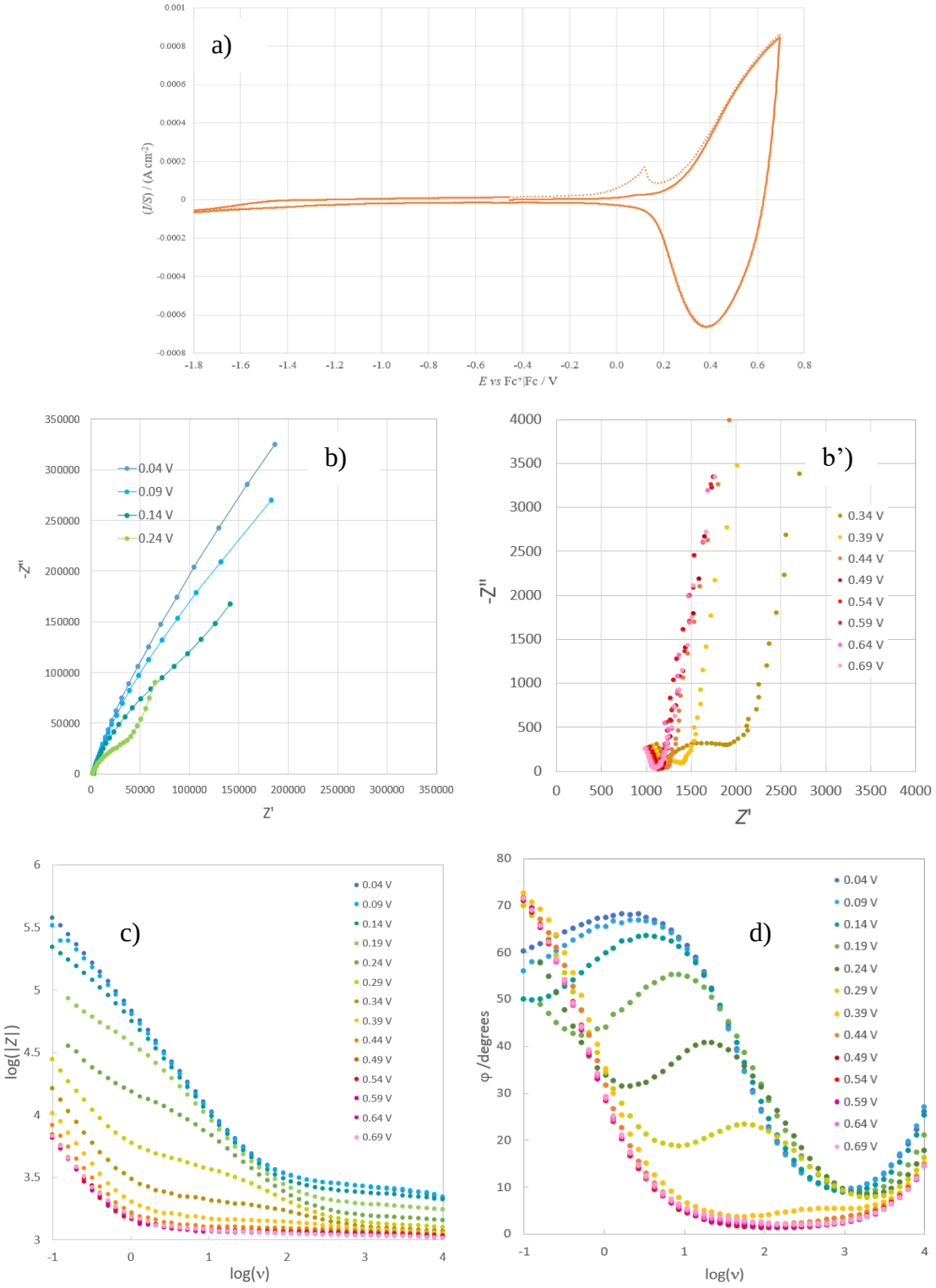

Figure S35. Features of a **[(2-BiTh)$_2$TT]$_n$** film electrodeposited on a GC electrode in CH_2Cl_2 with 0.1 M $TBAPF_6$ supporting electrolyte with a slightly different protocol (10 potential cycles at 0.05 V/s scan rate, larger potential cycle range) respect to the examples in Figure 9 in the main pape and former Figure S34 Top: stability cycle and charge trapping. Middle/bottom: impedance characteristics at increasingly positive polarizations, as Nyquist (b,b'), Bode modulus (c) and Bode phase diagrams (d).

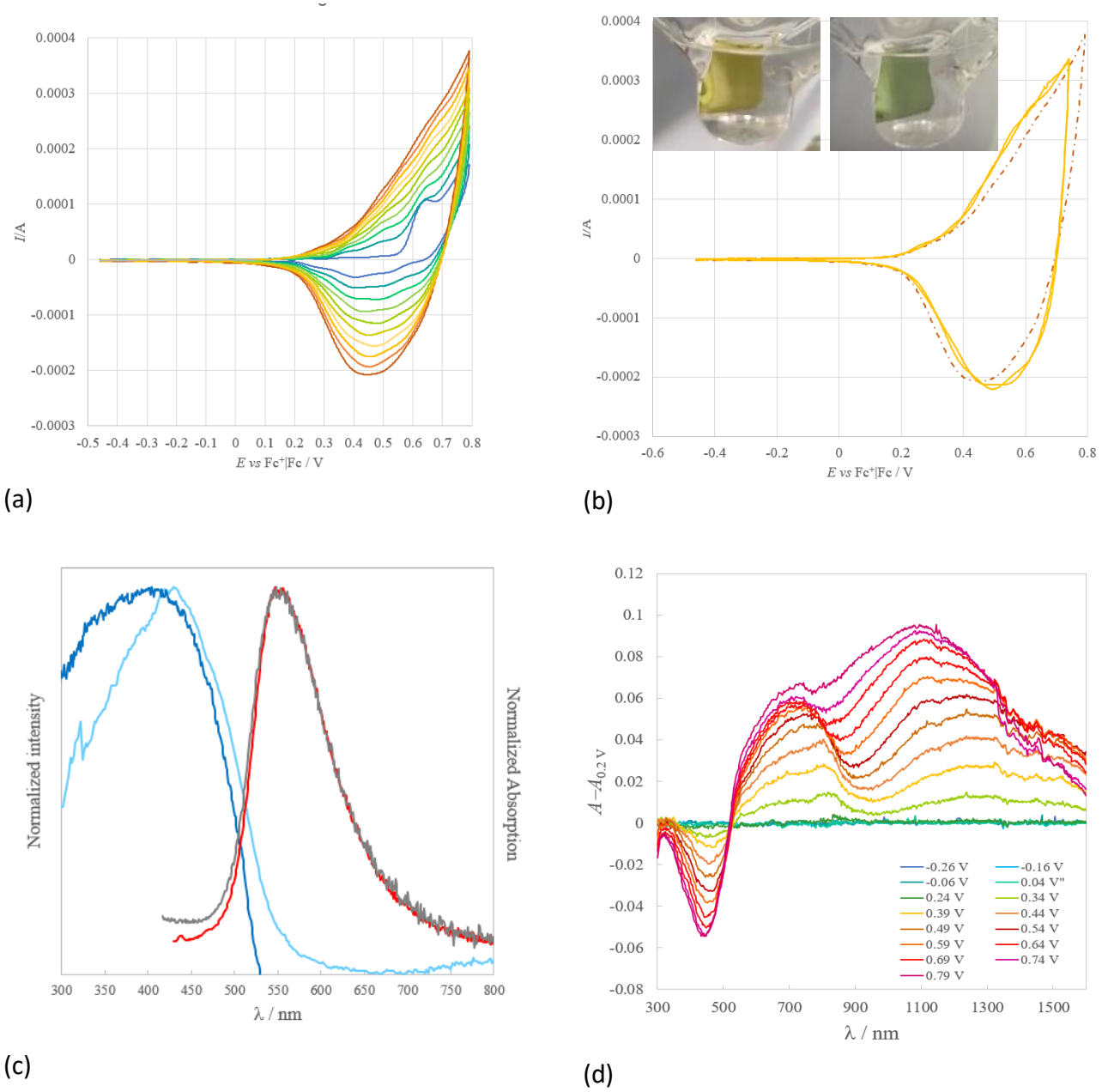

Figure S36 Features of **[(2-BiTh)$_2$TT]$_n$** films electrochemically formed on ITO electrode with a slightly different protocol (0.05 V/s scan rate, larger potential cycle range) respect to the examples in Figures 10 and 11 in the main paper. (a) Potentiodynamic electrodeposition in ~0.00075 M monomer solution in CH_2Cl_2 + 0.1 M $TBAPF_6$, (b) first and fourth stability cycle in monomer-free solution, and electrochromism (c) A synopsis of UV-Vis absorption (cyan line), excitation (λ_{em} 552 nm blue line) and emission (λ_{exc} 350 nm dark grey line; λ_{exc} 410 nm red line) spectra of an uncharged film on ITO electrode. (d) Differential UV-Vis /NIR spectra for a film deposited on ITO electrode, polarized at increasing potentials referred to Fc+|Fc in CH_2Cl_2 + 0.1 M $TBAPF_6$.